Chapter 5

Anti-proliferative activity, Molecular Docking and inhibition of Human Dihydrofolate reductase enzyme shown by Quinazoline-4(3H)-ones

Chapter 5

Anti-proliferative activity, Molecular Docking and inhibition of Human Dihydrofolate reductase enzyme shown by Quinazoline-4(3H)-ones

5.1 Introduction

Cancer is considered as one of the major clinical and public health problem. Cancer may be defined in three phases (i) aggressive- cells can grow and divide without respect to normal restrictions, (ii) invasive - adjacent tissues can be invaded and destroyed and/or (iii) metastatic - spread to further locations in body (Baba *et al.*, 2007). Conversely, benign tumors are self-limited in their growth and do not invade or metastasize and differentiate them from malignant properties of cancer. Cancer is known to affect people at all ages, even fetuses, but possibilities for the more common varieties have a tendency to increase with age. At present, cancer is considered as a leading cause of death worldwide. It is reported that in 2008 about 13% of all deaths (accounted for 7.6 million deaths) occurred due to cancer and more than 70% of all deaths occurred in low and middle income countries. It is now counted among five leading causes of death (American Chemical society, 2007). Cancer morbidity reached upto nine million people worldwide by 2015. Furthermore, deaths from cancer worldwide are projected to rise over 11 million in 2030 as per WHO Cancer Fact sheet No 297 February 2011. It is well known that conventional anticancer drug discovery and development processes have selected agents that had significant cytostatic or cytotoxic activity on tumour cell lines. The drug discovery was mainly focused on development of cytotoxic agents. These agents play a vital role in inhibiting metabolic pathways critical to cell division (Florea *et al.*, 2011).

The advances in history of cancer chemotherapy are shown in Figure 5.1, where most popular and effective drug methotrexate and 5-flurouracil were invented in 1950-60. With the current chemotherapy, lack of selectivity of chemotherapeutic agents against

cancerous cells is a significant problem. However, advances in the fields of drug discovery and cell biology are facilitated by the developments of Computer-Aided Drug Design. To facilitate the discovery of novel therapeutic agents, Computer-Aided Drug Design (CADD) assist to discover novel chemical entities with the potential to be developed into novel therapeutic agents. Thus, modern computational-aided drug design established a novel platform by which researchers perform in-depth *in silico* simulation prior to labour-extensive wet-lab validation (Zhang, 2009).

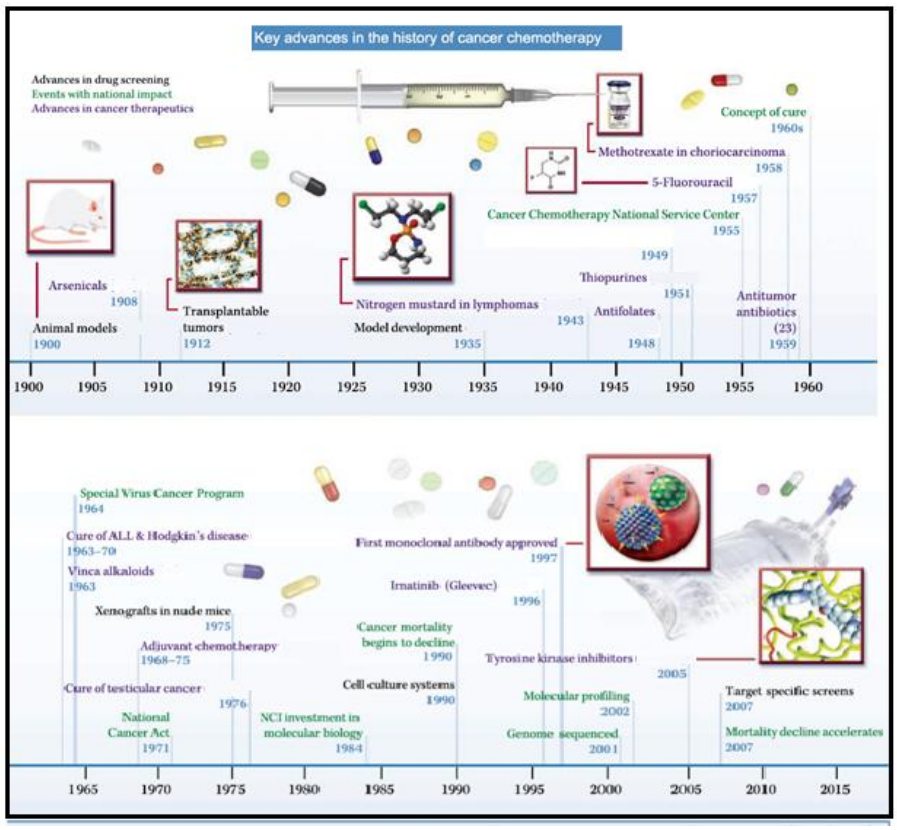

Figure 5.1: Representation of the key advances in the history of cancer chemotherapy.

5.1.1 Computer Aided Drug Design

5.1.1.1 Importance of computer-aided-drug design in medicinal chemistry

The strategy of medicinal chemists in their research is to discover new chemical entities which maximally resemble existing drugs with respect to key physicochemical and biological properties, with the knowledge that the quest for 'drug-like' properties may indeed help achieve good pharmacokinetic and pharmaco-dynamic properties **(**Hughes, 2011**).** In this regard, Computer-aided drug design plays a vital role in drug discovery and development and has become an indispensable tool in the pharmaceutical industry. Computational medicinal chemists can take advantage of all kinds of software and resources in the computer-aided drug design field for the purposes of discovering and optimizing biologically active compounds (Liao *et al.,* 2011). Thus, Computer-aided drug discovery/design methods have played a major role in the development of therapeutically important small molecules for over three decades.

5.1.1.2 Evaluation of Drug likeliness and ADME/Tox

In silico prediction of properties like, absorption, distribution, metabolism and excretion (ADME) by employing theoretical models play progressively more important roles in support of the drug development process (Hou & Wang, 2008). The importance of optimizing the ADME properties has been widely recognized in determining potential drug candidates. Generally, the evaluation of a drug is determined not only by good efficacy and specificity, but also by having acceptable ADME and toxicity properties (ADMET) (Tetko *et al.,* 2006). At the early stage , ADME predictions generally center on simple ADME or ADME-related properties, such as octanol-water partitioning coefficient (logP), apparent partition coefficient (log D), intrinsic solubility (logS), etc. and more complex ADME properties such as human intestinal absorption, blood-brain partitioning, oral bioavailability, clearance, volume of distribution and metabolism (Hou *et al.,* 2008). To exercise a pharmacological effect in tissues, a compound has to penetrate various physiological barriers, such as the blood–brain barrier, gastrointestinal barrier, and the microcirculatory barrier, to reach the blood circulation. Thereafter, it is

transported to its effectors site for distribution to tissues and organs, degraded by specialized enzymes, and finally removed from the body *via* excretion. The character of a pharmaceutical compound may be described by its pharmacokinetic or ADME properties (Tetko *et al.,* 2006). In addition, genetic variation in drug metabolizing enzymes implies that some compounds may undergo metabolic activation and cause adverse reactions or toxic in humans (Gardiner & Begg, 2006).

Accordingly, the ADME/Tox properties of a compound directly influence its usefulness and safety. The membrane permeability of a compound is determined by a combination of factors including compound size, aqueous solubility, ionizability (pKa) and lipophilicity (log P). The solubility of a neutral compound or of a compound in its non-ionized form is defined as the intrinsic solubility and normally represented as logs (Hou & Wang, 2008). In practice, about 85% of drugs have logs between -1 and -5. Christopher Lipinski carefully studied the physico-chemical properties of 2245 drugs from the World Drug Index (WDI) and found that poor absorption and permeation are more likely to occur when molecular weight <500 g/mol, Clog P< 5, hydrogen bond donors <5 and hydrogen bond acceptors <10 . A 'rule of five' was subsequently proposed with respect to drug likeness. He defined "drug-like" molecules as those that met 3 out of 4 of the following rules: a molecular weight ≤ 500 Da, ≤ 5 hydrogen bond donors, ≤ 10 hydrogen bond acceptors, the sum of N's and O's ≤10 and a ClogP ≤ 5 (MlogP ≤ 4.15) (Lipinski *et al.,* 1997). These rules were extended by other researchers, including Ghose *et al* (1999) and Oprea (2000). However, these rules could only serve as the minimal criteria for evaluating drug-likeness. It has been estimated that 68.7% of compounds in the Available Chemical Directory (ACD) Screening Database (2.4 million compounds) and 55% of compounds in ACD (240 000 compounds) do not violate the 'rule of five' (Hou *et al.,* 2006). It has been reported that the polar surface area (PSA) inversely correlates with the lipid penetration ability (Palm *et al.,* 1997). Compounds that are completely absorbed by humans tend to have PSA values of 60A˚, while compounds with PSA >140A˚ are less than 10% absorbed.

A molecular property is a complex balance of various structural features which determine whether a particular molecule is similar to the known drugs (Lilith *et al.,* 2010). It generally means "molecules which contain functional groups and/or have physical properties consistent with most of the known drugs". These properties, mainly hydrophobicity, molecular size, flexibility and presence of various pharmacophoric features influence the behavior of molecules in a living organism, including bioavailability. Computational chemists have a wide array of tools and approaches available for the assessment of molecular diversity. Diversity analysis has been shown to be an important ingredient in designing drugs. The computational sensitivity analysis and structural analysis have been used to study the drug-likeness of the candidate drug (Mohammed *et al.,* 2010; Mohammed *et al.,* 2011). Therefore, these drug-likeness filters or rules may be useful in the early stage of drug discovery to some extent while they should be used cautiously.

5.1.1.3 Evaluation of Interaction of Drug with target enzyme/receptor

Computer-Aided Drug Design (CADD) also included use of computational methods to simulate drug-receptor interactions. Molecular docking has become an increasingly important tool for drug discovery. Generally, docking is a computational technique that places a small molecule (ligand) in the binding site of its macromolecular target (receptor) and estimates its binding affinity (Yuriev *et al.,* 2011) (Figure 5.2). Many forces are involved in the intermolecular association: hydrophobic, dispersion, or van der Waals, hydrogen bonding, and electrostatic. The major force for binding appears to be hydrophobic interactions, but the specificity of the binding appears to be controlled by hydrogen bonding and electrostatic interactions (Ramesh *et al.,* 2012). The process of docking a ligand to a binding site tries to mimic the natural course of interaction of the ligand and its receptor *via* a lowest energy pathway (Ferreira *et al.,* 2015).

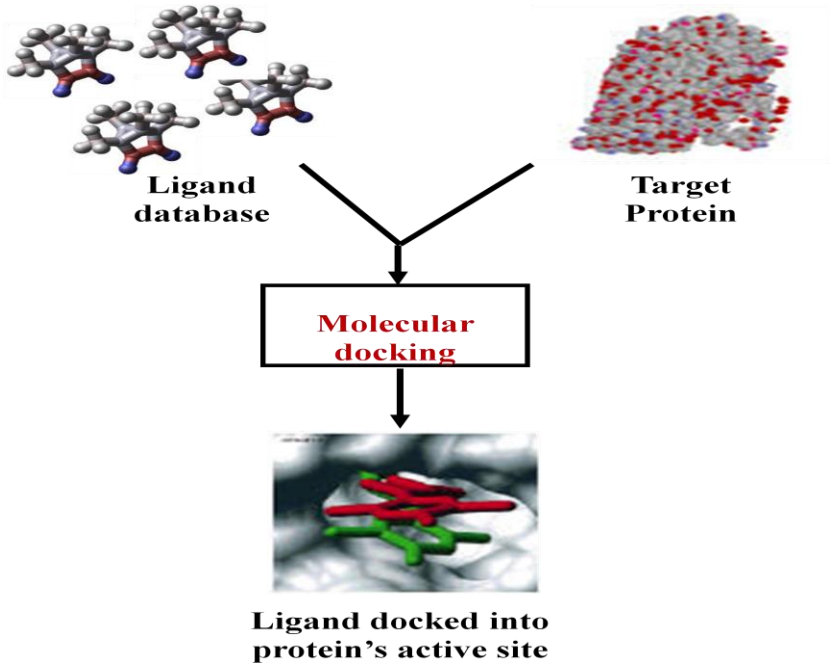

Figure 5. 2: Schematic representation of molecular docking.

5.1.2 Dihydrofolate reductase (DHFR)

Human dihydrofolate reductase (hDHFR) is one of the best therapeutic targets for the anticancer drug because of its metabolic importance. In the context of DHFR inhibitor, Farber used folate analogues for the treatment of acute lymphoblastic leukemia in 1948 (Farber, 1948). Further, in 1958, it was reported that folate analogues showed antitumor activity by inhibition of the dihydrofolate reductase (Osborn, 1958; Osborn & Huennekens, 1958).

Dihydrofolate reductase (DHFR; tetrahydrofolate dehydrogenase; 5, 6, 7, 8-tetra-hydrofolate-NADP$^+$ oxidoreductase; EC 1.5.1.3) is an enzyme of pivotal importance in biochemistry and medicinal chemistry. DHFR functions as a catalyst for the reduction of dihydrofolate to tetrahydrofolate. Reduced folates are carriers of one-carbon fragments; hence they are important cofactors in the biosynthesis of nucleic acids and amino acids (Roth, 1986). The inhibition of DHFR leads to partial depletion of intracellular reduced folates with subsequent limitation of cell growth (Nerkar *et al.*, 2009). DHFR has attracted attention of protein chemists as a model for the study of enzyme structure/

functional relationships. The species-differences among the DHFRs, **(**Falco *et al.,* 1949**)** were used to discover compounds with particular selectivity, e.g., that are lethal to bacteria but relatively harmless to mammals (Buchall & Hitchings, 1965). Such selective inhibitors are trimethoprim and pyrimethamine, which are used in therapy for their antibacterial and antiprotozoal properties, respectively. The enzymatic reduction involved in the inhibition of DHFR is a random process in which either the substrate (dihydrofolate) or the cofactor NADPH, forms a binary complex with the enzyme, with subsequent rapid binding of the inhibitor, to form ternary complex. Good amounts of work were done regarding inhibitors of DHFR (Blancey *et al.,* 1984).

Compounds that inhibit DHFR exhibit an important role in clinical medicine as exemplified by the use of methotrexate in neoplastic diseases (Jolivet *et al.,* 1983; Borst & Quellette, 1995), inflammatory bowel diseases (Kozarek *et al.,* 1989) and rheumatoid arthritis (Weinblatt *et al.,* 1985), as well as in psoriasis (Weinstein, 1971; Abu-Shakra, 1995) and in asthma (Mullarkey *et al.,* 1988) like that of trimethoprim in bacterial diseases (Green *et al.,* 1984). Lately, a new generation of potent lipophilic DHFR inhibitors such as trimetrexate (TMQ) and piritrexim (PTX) have shown antineoplastic (Maroun, 1988) and most importantly, antiprotozoal (Allegra *et al.,* 1987) activities. This is the exclusive *de novo* sources of dTMP, hence inhibition of DHFR or TS activity in the absence of salvage, leads to "thymine-less death **(**Masur, 1990; Berman, Werbel *et al.,* 1991). Thus DHFR inhibition has long been an attractive goal for the development of chemotherapeutic agents against bacterial and parasitic infections as well as cancer (Borst *et al.,* 1995).

5.1.3 Inhibitors of Dihydrofolate Reductase

Inhibitors of DHFR are classified as either classical or non-classical antifolates (Al-Rashood *et al.,* 2014). The classical antifolates are characterized by a *p*-aminobenzoylglutamic acid side-chain in the molecule and thus closely resemble folic acid itself. Methotrexate (MTX) is N-{4-[[(2, 4-diamino-6-pteridyl) methyl]-N^{10}-methyl-amino]} benzoyl-glutamic acid, the most well known drug among the classical antifolates. Compounds classified as non-classical inhibitors of DHFR do not possess the

p-aminobenzoylglutamic acid side-chain but rather have a lipophilic side-chain (Green *et al.*, 1984).

5.1.3.1 Classical DHFR Inhibitors

The classical inhibitor serves as an antimetabolite, which means that it has a similar structure to that of a cell metabolite, resulting in a compound with a biological activity that is antagonistic to the metabolite. In case of folic acid, MTX, most often used DHFR inhibitor in clinic today, is antagonistic to folic acid. The antibacterial drug trimethoprim is generally used together with the TMP (Al-Rashood, 2005). The most common use of MTX is as an anticancer drug. It inhibits the synthesis of metabolites involved in one-carbon unit transfer reactions such as the biosynthesis of the important nucleotides. Moreover, MTX is considered as a competitive and reversible inhibitor of DHFR that binds tightly to the hydrophobic folate-binding pocket of the enzyme. The affinity of MTX for DHFR increases considerably in the presence of the cofactor NADPH and have anti-inflammatory and immuno-suppressive properties with accompanied activity against autoimmune disorders (Graffner-Nordberg, 2001).

5.1.3.2 Non-classical DHFR Inhibitors

The clinically useful properties of MTX have stimulated the quest for a variety of new analogues with modifications within the molecule, without interfering too much with the pharmacophore of the original drug. Intrinsic and acquired resistance to MTX and other antifolate analogues limit their clinical efficacy. Thus, research is enduring for a more selective drug, most importantly, without the severe side-effects often associated with MTX (Jolivet *et al.*, 1983). New more lipophilic antifolates have been developed in an attempt to circumvent the mechanisms of resistance, such as decreased active transport, decreased polyglutamation, DHFR mutations etc (Urakawa *et al.*, 2000). These modified antifolates differ from the traditional classical analogues by increased potency, greater lipid solubility, or improved cellular uptake.

In this study we have tried to investigate the antiproliferative potential of some 3-(Aryldeneamino)-2-phenyl-quinazoline-4(3H)-ones via inhibition of hDHFR. Computational approaches have demonstrable capability to play an important role in this endeavour.

5.2 Materials and methods

5.2.1 Chemicals

Chemicals used are: Anthranilic acid (Sigma Aldrich India), pyridine, anisaldehyde, salicylaldehyde, 3-(4, 5- dimethylthiazol-2-yl)-2,5-diphenyltetrazolium bromide (MTT), p-nitro blue tetrazolium/5-bromo-4-chloro-3-indolyl phosphate system (NBT-BCIP) (SRL, India).

Cell lines were obtained from NCCS Pune, India. Dulbecco's Modified Eagle Medium (DMEM), fetal bovine serum (FBS), penicillin streptomycin neomycin (PSN) antibiotic, trypsin and ethylenediaminetetraaceticacid (EDTA) were obtained from Gibco BRL (Grand Island, NY, USA). Tissue culture plastic wares were obtained from NUNC (Roskidle, Denmark) and Bradford protein assay reagent from Fermentus, EU. DAPI (4', 6-diamidino-2-phenylindole dihydrochloride), acridine orange (AO), and ethidium bromide (EtBr) were procured from Invitrogen, California.

5.2.2 Maintenance of Cell culture

MCF-7 (Human breast adenocarcinoma), HepG2 (Human hepatocellular carcinoma), and HeLa (Human cervical cancer) cells were cultured in DMEM supplemented with 10% fetal bovine serum (FBS) and 1% antibiotic penicillin , streptomycin and Neomycin (PSN) at 37°C in a humidified atmosphere under 5% CO_2. After 75-80% confluency, cells were harvested with 0.025% trypsin and 0.52 mM EDTA in phosphate buffered saline (PBS), and seeded at desired density to allow them to re-equilibrate a day before the start of experiment.

5.2.3 Molecular Docking

The study comprised compounds belonging to quinazoline-4-(3H)-ones (Figure 5.3) along with one standard drug methotrexate. The selected compounds have different substituents as shown in Table 5.1.

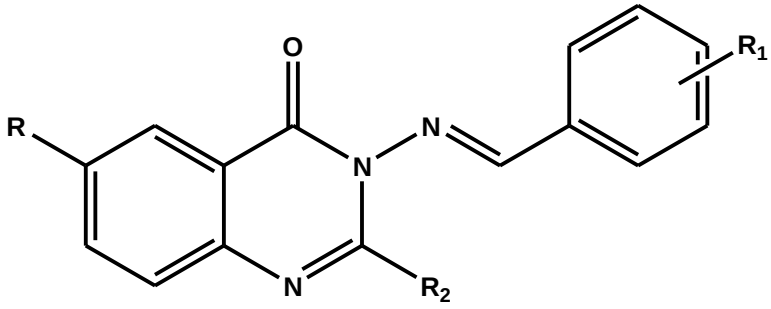

Figure 5.3. Structure of 3-amino-2-aryl-4(3H)-quinazolinone

Table 5.1- The substituents of the 3-amino-2-aryl-4(3H)-quinazolinone

Compounds	R	R^1	R^2
3a	H	2-OH	Ph
3b	H	4-OCH3	Ph
3c	H	4-F	Ph
3d	H	4-N(CH3)2	Ph
3e	H	4-Cl	Ph
3f	H	3-OCH3	Ph
3g	H	4-OH	Ph
3h	H	3-OCH3, 4-OH	Ph
3i	H	3-NO2	Ph
3j	H	H	Ph
4a	H	3,5-Cl	Ph
4b	H	3-NO2-4-Cl	Ph
4c	H	4-CF3	Ph
4d	H	3-Cl	Ph
4e	H	2,3-Cl	Ph
4f	H	2,6-Cl	Ph

4g	H	3,4-F	Ph
4h	H	3-CF3	Ph
4i	6-Br	2-F	Me
4j	6-Br	3-F	Me
4k	6-Br	4-F	Me
4l	6-Br	2-CF3	Me
4m	6-Br	3-Cl	Me
4n	6-Br	2,4-Cl	Me
4o	6-Br	2,6-Cl	Me
4p	6-Br	3,4-F	Me
4q	6-Br	2-Cl-5-NO2	Me
4r	6-Br	4-Cl-3-NO2	Me
4s	6-Br	2-F-3-CF3	Me
4t	6-Br	3,4-OMe	Me
4u	6-Br	2,3-OMe	Me
4v	6-Br	2,5-OMe	Me
4w	6-Br	3-NO2	Me
4x	6-Br	2-OH	Me
4y	6-Br	2,4-OMe	Me
4z	6-Br	5-Cl-3-OH	Me
4	H	2,3-Cl	Me

5.2.3.1 Chemical Drawing

The structure of the compounds was drawn by software ACDLabs Chemsketch 12.0. The created structures were energy minimized by 3D viewer in ACDLabs and the corresponding structures were saved as MDL.mol file format.

These files were opened in ArgusLab 4.0 software and energy minimization of each of the structure was done by using UFF calculation. The respective structures were then saved as the .pdb file format for the further study.

5.2.3.2 Molecular Docking

In order to carry out the molecular docking study, we used the AutoDock 4.0 suite as molecular-docking tool (Morris *et al.,* 1998). It is suitable software for performing automated docking of ligands to their macromolecular receptors. Protein- ligand softwares were widely used to support the drug design process.

5.2.3.3 Preparation of Human DHFR

The basic requirement of the docking is the identification of appropriate target protein. We have chosen Human Dihydrofolate Reductase (PDB ID 1DHF) which fulfills all the requirements of this study. It was retrieved from the PDB structural database site (http://www.rcsb.org/pdb). The .pdb file format of protein was taken as input of Autodock program. All water molecules and ligands were removed from the proteins before the docking procedure. The protein was modified using the AutoDock program through which all missing hydrogen, side chain atoms added and residues repairing were done by using the graphic user interface of AutoDock tools (ADT).

5.2.3.4 Preparation of Ligands

The .pdb file format of ligands was used for the docking. The docking input files of ligands were also prepared using ADT package. Similarly ‘‘.pdb’’ file of ligand was given as input to modify ligand file which allowed the program to calculate its parameters such as non-polar hydrogen, aromatic carbons and rotatable bonds along with the ligand torsions. The Torsion count option was used to adjust the number of rotatable and non-rotatable bonds. For all the ligands Torsions were defined by the use of Torsion Tree option from the AutoDock software. The Torsion Tree option was used to Choose Torsions, Set Number of Torsions to most atoms and to Detect Root which is the rigid part of the ligand. The number of active

torsions was set to the maximum number of atoms. Ligands were saved as .pdbqt file format.

5.2.3.5 Grid box preparation

AutoDock requires pre-calculated grid maps, one for each atom type, present in the ligand being docked and its stores the potential energy arising from the interaction with macromolecule. This grid must surround the region of interest in the macromolecule. In the present study, the binding site was selected based on the amino acid residues, which are involved in folate binding. . Therefore, the grid was centered in the active region of hDHFR motif and includes all amino acid residues that surround active site. The grid box size was set at 90, 90, and 90 A° (x, y, and z), though it was changed depending on the ligand size. AutoGrid 4.0 Program, supplied with AutoDock 4.0 was used to produce grid maps. The preparation steps were started by using .pdb file of human DHFR as the receptor, and its ligand. Grid Box is the coordinate area determination for the docking process. It is configured in AutoDock Tools. Using MGLTools 1.5.1., the grid was centered on the active site of the enzyme for docking. The grid box was saved in a grid parameter file (.gpf) format.

5.2.3.6 Docking simulation

During the docking process, a maximum of 10 conformers was considered for each compound. Docking for 10 number of GA run was carried out using Lamarckian Genetic Algorithm (LGA) and all other parameters set to default. The top ranked model in the lowest energy cluster with maximum cluster size was considered for all further interaction studies. This process was done using AutoGrid 4.0 and Autodock 4.0. The following data are necessary for conducting the docking: enzyme file in .pdbqt format, ligand in .pdbqt format, .gpf files, and .dpf files.

5.2.3.7 Analysis and visualization of docking simulation results

The docking result of AutoDock 4.0 is in the docking log file (.dlg) format. Then, by using python script, the docking results were converted to .pdb format. Out

of 10-model result, one best model was picked up, based on the free energy bonding data, in order to analyze its interaction.

5.2.4 *In silico* Physicochemical and Drug likeliness Tests

Drug-likeliness is mostly a statistics of descriptors derived from databases of compounds used to evaluate the drug-likeliness of other compounds. The web server which predicted the (1) CMC like rule which is based on databases contain more than 7000 compounds, used or tested as medicinal agents in humans. (2) MDDR contained more than 10000 drugs launched or under development (3) The WDI 1997 contains 51596 compounds for comparing the drug-likeliness and also by the Lipinski rule of five. Drug likeliness was calculated using OSIRIS server, which is based on a list of about 5,300 distinct substructure fragments created by 3,300 traded drugs as well as 15,000 commercially available chemicals yielding a complete list of all available fragments with associated drug likeliness.

The physical characteristics of all the molecules were determined because the biological properties could be predicted by their physicochemical property. Molinspiration supported internet benefitted the chemistry community by offering free on-line services for calculation of important molecular properties (LogP, polar surface area, number of hydrogen bond donors and acceptors and others). Any compound to be considered as a lead must possess acceptable scores for all of the descriptors and Osiris Property explorer http://www. organic-chemistry.org/prog/peo/ were used to calculate - logP, solubility, drug likeliness, polar surface area, molecular weight, number of atoms, number of rotatable bonds, volume, drug score and number of violations to Lipinski's rule The cLogP, solubility, drug likeness and drug Score of each molecule were also determined by OSIRIS server.

Computer aided method is an easy platform to search such kinds of biologically active compounds with favorable ADMET (Absorption, Distribution, Metabolism, Excretion and Toxicity) and drug-likeness properties**.** The ADME are the most important part of pharmacological studies of the concerned molecule required for drug based discovery. Pre ADMET is the tool that provides drug-

likeliness, ADME profile and toxicity analysis for the ligand. It uses Caco2-cell (heterogeneous human epithelial colorectal adenocarcinoma cell lines) and MDCK (Madin-Darby Canine Kidney) cell models for oral drug absorption prediction and skin permeability, and human intestinal absorption model for oral and trans-dermal drug absorption prediction. Distribution is predicted using BBB (blood brain barrier) penetration and plasma protein binding.

5.2.5 Inhibitory toxicity prediction

The Osiris program was used to predict the overall toxicity of the most active derivatives as it may point to the presence of some fragments generally responsible for the irritant, mutagenic, tumorigenic, or reproductive effects in these molecules.

5.2.6 Pharmacophore generation

The compounds were structurally aligned to get a ligand based pharmacophore using PharmaGist tool (Schneidman-Duhovny et al, 2008). A ligand-based pharmacophore modeling was performed using PharmaGist webserver. The method consists of four major steps: (i) ligand representation, (ii) pairwise alignment, (iii) multiple alignments and (iv) solution clustering and output as shown in Figure 5.4. In a common pharmacophore development approach, large number of possible conformations for each ligand were generated, whereas PharmaGist uses the most active compound as 'the pivot' that is considered within the search for the common pharmacophore. The benefit of this approach lies in the fact that when there is no information on the binding conformation of any of the ligands, a set of conformations for only one of them (the pivot) needs to be computed. Unless a pivot is specified by the user, the algorithm iteratively tries each input ligand as a pivot. The algorithm identifies pharmacophores by computing multiple flexible alignments between the input ligands. The resulting multiple alignments reveal spatial arrangements of consensus features shared by different subsets of input ligands. The highest-scoring ones are potential pharmacophores (Dror *et al.,* 2009). Ten active compounds (Table 5.1) from the series were selected to generate pharmacophore models. Compound 11 was assigned as the pivot molecule and default values were used for other settings. Models with all the 10 ligands with contribution to

the pharmacophoric features were considered. Generated models were ranked with the scores and the one with highest score was selected as the best pharmacophore model.

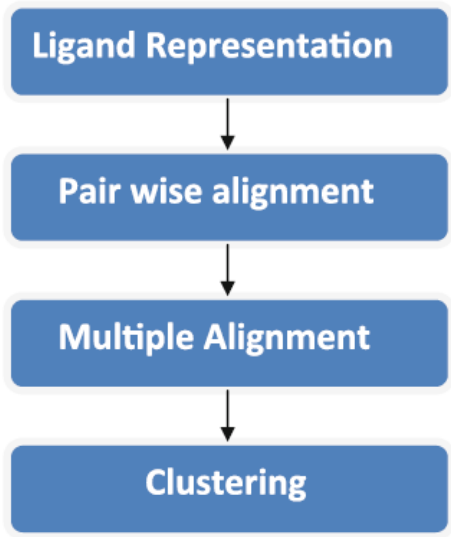

Figure 5.4: Flow-chart of PharmaGist method

5.2.7 hDHFR activity assay

hDHFR activity was measured using the DHFR assay kit (Sigma-Aldrich-CS0340) as per the manufacturer's instructions. Typically, DHFR activity is measured using a Jasco V spectrophotometer to quantify the decrease in absorbance at 340 nm for every 5 s over 2.5 min. The stock solutions for the reaction mixture was Methotrexate (1×10^{-6}M) , NADPH (1×10^{-3}M), DHF (1×10^{-3}M) and synthesized compounds (10^{-6}M). DHFR activity was determined by measuring the decrease of absorbance at 340 nm characteristic of dihydrofolate as it is reduced to tetrahydrofolate (THF). The activity calculation measures the decrease in OD obtained during 2.5 min. The output of the kinetics program was ΔOD/min.

$$Inhibition\ \% = \frac{Activity\ of\ DHFR\ in\ presence\ of\ inhibitor}{100} \text{X}\ Activity\ of\ DHFR\ in\ presence\ of\ inhibitor$$

The % inhibition values were plotted versus drug concentration (log scale). The 50% inhibitory concentration (IC_{50}) of each compound was obtained.

5.2.8 MTT assay

Stock solutions of synthesized compounds and standard compounds (methotrexate and curcumin) at a concentration of 10 mg/ml were prepared in dimethyl sulfoxide (DMSO, Hi-Media). The cytotoxic effect of each of compound was evaluated by tetrazolium- dye, MTT, assay (Mosmann, 1983; Denizot & Lang, 1986) with slight modifications. Briefly, the cancerous cells (MCF 7, $HepG_2$ and HeLa) were seeded in 96-well plates at a density of $5x10^3$ cells/well in 200 µl culture medium. Following 24 h incubation and attachment, the cells were treated with different concentrations of compounds and similar concentration of diluents (DMSO) for further 24 h. After treatment, media was replaced with MTT solution (10 µl of 5 mg/ml per well) prepared in PBS and incubated for 3 h at 37 ^oC in a humidified incubator with 5% CO_2. The yellow MTT dye was reduced by succinate dehydrogenase in the mitochondria of viable cells to purple formazan crystals. To solubilize the formazan, 50 µl of isopropanol was added to each well. The plates were gently shaken for 1 min and absorbance was measured at 600 nm, with reference 490 nm, by microtiter plate reader (MIOS Junior, Merck). The percentage of cytotoxicity was calculated as (Y-X)/Y x 100, where Y is the mean optical density of control (DMSO treated cells) and X is the mean optical density of treated cells with compounds.

5.2.9 Assessment of cell morphology

Cells (3×10^4/well) grown in 6-well plates in DMEM supplemented with 10% FBS for 24 h were treated with or without derivatives. Cells were seeded in 35 mm polyvinyl coated cell culture plates and allowed to attach at 37 ^0C for 24 h in CO_2 incubator. The following day, cells were treated with either 75 µg/ml of compounds or DMSO alone, serving as control, and incubated again at the same conditions. The morphological changes of cancerous cells under treatment and control conditions were compared by monitoring with phase contrast inverted microscope (Olympus, CK40-SLP) at 200X magnification. The images were photographed at 24 h of incubation.

5.2.10 Trypan blue exclusion assay

After morphological assessment, the cell viability was simultaneously assessed by Trypan blue dye exclusion assay (Strober, 1992). For this, the cells were trypsinized with 0.25% trypsin-EDTA solution, resuspended in phosphate buffer saline (PBS) and stained with 0.4% Trypan bluedye solution (v/v in PBS). Within two minutes, the cells were loaded in a Neubauer chamber and the number of viable and non-viable cells per 1 x 1 mm square was counted under phase contrast microscope. The dead cells, because of losing the semi permeability of membrane, retained the blue dye and hence are colored whereas viable or live cells remained unstained. The cells/ml was calculated as average cell count x dilution factor x 10^4 cells/ml. The % cell viability was determined as [(no. of viable cells/ total no. of viable + non-viable cells) x 100. The percentage of growth inhibition was represented as {cell viability (control) – cell viability (with test compound).

5.2.11 Statistical analysis

All values are expressed as mean ± SD. Statistical significance was compared between various treatment groups and controls using the one-way analysis of variance (ANOVA). Data were considered statistically significant when P values were <0.01.

5.3 Results and Discussion

In the last few years, the attention was oriented towards the synthesis and biological evaluation of quinazolinone derivatives as they exhibit a broad spectrum of biological activities. Moreover, there is an increasing interest in finding novel field of applicability for Quinazoline-4(3H)-one compounds as anticancer drugs. Importantly, FDA has approved several quinazoline derivatives as anticancer drugs from the past 15 years, such as gefitinib, erlotinib and lapatinib (Roskoski *et al.*, 2014).

5.3.1 Drug likeliness of compounds

Apart from advances in technology and understanding of biological systems, drug discovery is still a long process with low rate of new therapeutic discovery. Fortunately, modern computational-aided drug design established a novel platform by which researchers perform in-depth *in silico* simulation prior to labor-extensive wet-lab validation. Hence we have chosen first to perform *in silico* evaluation of compounds' drug likeliness behaviour (physicochemical properties, interaction with target protein, ADMET and drug score) and their possibility to become a drug in future

All the ten compounds used in this study were allowed to pass through different parameters required to fulfill the candidature of these compounds as future drug. In addition to these ten 3-(Aryldeneamino)-2-phenyl-quinazolin-4(3H)-one, we have computationally constructed twenty seven more quinazolinone compounds, which are reported for their biological activity (Xingwen *et al.*, 2007). This approach was also taken to verify dependability of the applied tools and softwares. All compounds (synthesized and computationally constructed) have successfully qualified Lipinski's Rules, CMC like rule (except 4a and 4f), MDDR like rule and WDI like rule (Table 5.2). Compounds tested in this study were predicted to have good oral bioavailability. Some of the compounds (4e, 4f and 4) have shown excellent permeability, while others have relatively less or poor (in some cases) permeability. The drug likeliness and drug score were found significant for all tested compounds.

The suitability of a promising drug also depends on its toxicity. The therapeutic index of a drug would be higher when it shows low toxicity/side effects. Based on this we have performed toxicity prediction using Osiris Property Explorer. Results revealed that the compounds have low toxicity. The prediction using Osiris Property Explorer was shown in color codes. Green color represents low toxicity, yellow represents the mediocre toxicity, and red represents high toxicity (Table 5.3).

Table 5.2- Data representing the qualification of the substituents for drug likeliness using CMC like rule, MDDR like rule and WDI like rule along with Rule of Five as predicted using OSIRIS server

Compound	CMC like rule	MDDR like rule	Rule of five	WDI like rule
1a	Qualified	Mid structure	Suitable	90%
2a	Qualified	Mid structure	Suitable	90%
3a	Qualified	Mid structure	Suitable	90%
3b	Qualified	Mid structure	Suitable	90%
3c	Qualified	Mid structure	Suitable	90%
3d	Qualified	Mid structure	Suitable	90%
3e	Qualified	Mid structure	Suitable	90%
3f	Qualified	Mid structure	Suitable	90%
3g	Qualified	Mid structure	Suitable	90%
3h	Qualified	Mid structure	Suitable	90%
3i	Qualified	Mid structure	Suitable	90%
3j	Qualified	Mid structure	Suitable	90%
4a	Not qualified	Mid structure	Suitable	90%
4b	Qualified	Mid structure	Suitable	90%
4c	Qualified	Mid structure	Suitable	90%
4d	Qualified	Mid structure	Suitable	90%
4e	Qualified	Mid structure	Suitable	90%
4f	Not qualified	Mid structure	Suitable	90%
4g	Qualified	Mid structure	Suitable	90%
4h	Qualified	Mid structure	Suitable	90%
4i	Qualified	Mid structure	Suitable	90%
4j	Qualified	Mid structure	Suitable	90%
4k	Qualified	Mid structure	Suitable	90%
4l	Qualified	Mid structure	Suitable	90%

4m	Qualified	Mid structure	Suitable	90%
4n	Qualified	Mid structure	Suitable	90%
4o	Qualified	Mid structure	Suitable	90%
4p	Qualified	Mid structure	Suitable	90%
4q	Qualified	Mid structure	Suitable	90%
4r	Qualified	Mid structure	Suitable	90%
4s	Qualified	Mid structure	Suitable	90%
4t	Qualified	Mid structure	Suitable	90%
4u	Qualified	Mid structure	Suitable	90%
4v	Qualified	Mid structure	Suitable	90%
4w	Qualified	Mid structure	Suitable	90%
4x	Qualified	Mid structure	Suitable	90%
4y	Qualified	Mid structure	Suitable	90%
4z	Qualified	Mid structure	Suitable	90%
4	Qualified	Mid structure	Suitable	90%

Table 5.3: Toxicity prediction as per output of Orisis programme

Compound	**Mutagenic**	**Tumorogenic**	**Irritant**	**Reproductive effect**
1a	Green	Green	Green	Yellow
2a	Green	Green	Green	Yellow
3a	Green	Green	Green	Green
3b	Green	Green	Green	Green
3c	Green	Green	Green	Green
3d	Green	Green	Green	Green
3f	Green	Green	Green	Green
3g	Green	Green	Green	Yellow
3h	Green	Green	Green	Green
3i	Green	Green	Green	Green
3g	Green	Green	Green	Green
4a	Green	Green	Green	Yellow
4b	Green	Green	Green	Yellow
4c	Green	Green	Green	Yellow

4d	Green	Green	Green	Yellow
4e	Green	Green	Green	Yellow
4f	Green	Green	Green	Yellow
4g	Green	Green	Green	Yellow
4h	Green	Green	Green	Yellow
4i	Green	Green	Green	Green
4j	Green	Green	Green	Yellow
4k	Green	Green	Green	Green
4l	Green	Green	Green	Green
4m	Green	Green	Green	Green
4n	Green	Green	Green	Green
4o	Green	Green	Green	Green
4p	Green	Green	Green	Green
4q	Green	Green	Green	Green
4r	Green	Green	Green	Green
4s	Green	Green	Green	Green
4t	Green	Green	Green	Green
4u	Green	Green	Green	Green
4v	Green	Green	Green	Green
4w	Green	Green	Green	Green
4x	Green	Green	Green	Green
4y	Green	Green	Green	Green
4z	Green	Green	Green	Green
4	Green	Green	Green	Green

5.3.1.1 Molecular descriptor properties

The oral bioavailability of the compounds projected as potential drugs were evaluated by determining the molecular weight, number of rotatable bonds (nrotb), number of hydrogen bonds (nON and nOHNH), and drug's polar surface (TPSA) as shown in Table 5.4. Since the individual molecular weights of all the compounds were less than 500, the numbers of rotatable bond were <10, the number of hydrogen bond donors and acceptors were < 12, and TPSA values being <140, they qualified to be an ideal oral drug. Compounds tested in this study were also predicted to have good oral bioavailability.

Table 5.4. Molecular descriptor properties of compounds.

Compounds	miLogP	TPSA	nON	nOHNH	Nviolations	nrotb	volume	natoms
1a	3.2	43.10	4	0	0	1	195.84	17.0
2a	3.1	45.75	4	0	0	1	199.76	17.0
3a	5.7	65.26	4	0	0	1	327.87	25.0
3b	6.7	57.89	4	0	0	1	294.72	25.0
3c	3.9	45.03	4	0	0	3	315.87	23.0
3d	4.8	48.87	4	0	0	3	287.67	22.0
3e	4.5	45.03	4	0	0	2	298.0	26.0
3f	5.6	48.54	4	0	1	2	321.8	23.0
3g	5.8	49.87	4	0	0	3	318.9	24.0
3h	6.9	65.26	4	0	0	3	307.0	22.0
3i	5.2	58.92	4	0	0	3	305.0	25.0
3j	6.2	45.03	7	0	0	2	312.65	26.0
4a	5.887	47.26	4	0	1	3	321.37	27.0
4b	5.16	93.08	4	0	0	3	317.53	27.0
4c	4.25	47.26	4	0	0	3	288.64	25.0
4d	5.25	47.26	4	0	1	3	307.84	26.0
4e	5.863	47.26	4	0	1	3	321.37	27.0
4f	5.86	47.26	4	0	1	3	321.37	27.0
4g	4.85	47.26	4	0	0	3	304.17	27.0
4h	5.47	47.26	4	0	1	4	325.60	29.0
4i	3.47	47.26	4	0	0	2	262.27	22.0
4j	3.5	47.26	4	0	0	2	262.27	22.0
4k	3.52	47.26	4	0	0	2	262.27	22.0
4l	4.20	47.26	4	0	0	3	288.64	25.0
4m	4.01	47.26	4	0	0	2	270.88	22.0
4n	4.64	47.26	4	0	0	2	284.41	23.0
4o	4.62	47.26	4	0	0	2	284.41	23.0
4p	3.61	47.26	4	0	0	2	267.20	23.0

4q	3.92	93.08	7	0	0	3	294.21	25.0
4r	3.52	47.26	4	0	0	2	262.27	22.0
4s	4.32	47.26	4	0	0	3	293.57	26.0
4t	3.00	65.72	6	0	0	4	308.43	25.0
4u	3.18	65.72	6	0	0	4	308.43	25.0
4v	3.40	65.72	6	0	0	4	308.43	25.0
4w	3.2	93.08	7	0	0	3	280.67	24.0
4x	3.3	67.48	5	1	0	2	265.36	22.0
4y	3.40	65.72	6	0	0	4	308.43	25.0
4z	3.95	67.48	5	1	0	2	278.898	23.0
4	4.62	47.26	4	0	0	2	284.41	23.0

Calculation of the fragment based drug-likeliness of the compounds signifies that the compounds have the same fragments as compared to the existing drugs. The drug-likeliness values of all the compounds are reasonably acceptable (except 4h,4i and 4s) as shown in Table 5.5. The higher drug-likeliness values are found in case of compounds 4c, 4d, 4e and 4f. Results indicated that these four compounds have the most fragments similar to existing potent drugs to fulfill the content of drugs. The drug score values (Table 5.5) were also calculated which took into account the effect of drug-likeliness, LogP, solubility, molecular weight, and toxicity risk together.

Table 5.5. Fragment based drug-likeliness of the compounds.

Compound	cLogP	Solubility	MW	Drug likeness	Drug Score
1a	2.35	-3.34	223	1.84	0.51
2a	3.93	-3.06	237	1.11	0.6
3a	3.74	-4.5	341.0	5.27	0.67
3b	4.05	-4.82	355	5.04	0.61
3c	4.22	-5.11	343	2.59	0.56

3d	4.01	-4.84	368	5.99	0.61
3e	4.72	-5.54	359	6.03	0.43
3f	4.05	-4.82	355	5.4	0.61
3g	3.77	-4.6	341	5.37	0.66
3h	3.77	-4.5	371	5.27	0.67
3i	3.44	-4.88	370	5.39	0.65
3j	4.12	-4.8	325	5.21	0.62
4a	5.26	-6.27	393	1.71	0.23
4b	3.77	-5.44	404	5.07	0.45
4c	4.65	-5.44	393	5.19	0.4
4d	5.26	-5.54	359	5.51	0.31
4e	5.26	-6.27	394	5.59	0.4
4f	4.65	-6.27	394	6.1	0.31
4g	4.16	-5.43	361	2.68	0.42
4h	4.8	-5.58	393	-1.84	0.21
4i	3.42	-4.78	362	1.44	0.59
4j	3.42	-4.78	360	0.12	0.4
4k	3.42	-4.78	360	1.91	0.61
4l	4.12	-5.24	410	-6.99	0.27
4m	3.97	-5.2	376	2.72	0.55
4n	4.59	-5.2	411	3.17	0.44
4o	3.97	-5.94	411	3.76	0.56
4p	3.48	-5.09	378	0.19	0.47
4q	3.71	-5.84	421	1.5	0.45
4r	3.71	-5.84	428	3.16	0.49
4s	4.18	-5.56	402	-4.45	0.25
4t	3.15	-4.5	402	4.56	0.66
4u	3.15	-4.5	402	3.02	0.65
4v	3.15	-4.5	402	3.23	0.66
4w	3.09	-5.1	387	2.57	0.6

4x	3.06	-4.17	358	2.7	0.71
4y	3.15	-4.5	402	1.57	0.61
4z	3.67	-4.9	392	3.41	0.6
4	3.89	-5.1	332	4.94	0.49

Any compound that is considered to be a better drug candidate should exhibit better drug score. Our data showed that compound 4x has the best score (0.71), compounds (2a, 3b, 3c, 3d, 3f, 3g, 3i, 3j, 4t, 4v,4k,4i,4m,4o and 4y) in the range of 0.5-0.66 and rest of the compound in range of 0.2-0.5. The hydrophobicity of drugs could be inferred from LogP values (Table 5.5). It was found that hydrophobicity and retention time of drug inside the host are directly related *i.e.* higher the hydrophobicity, higher the retention time of the drug inside the body (Tambunan *et al.,* 2011).

5.3.1.2 ADME prediction

In modern drug designing process, computational approaches like preADMET prediction; MDCK and Caco-2 cell permeability, etc. serve as computational screening model for the prediction of intestinal drug absorption. All the compounds under study have qualified HIA%, *in vitro* plasma% (>90% in all the cases) and Caco-2 cell permeability (>25 nm/sec) to be good drug candidate. Some of the compounds have shown excellent permeability, while others have relatively less or poor (in some cases) permeability in relation to qualify as CNS drug and MDCK permeability as shown in Table 5.6. Less permeability may have been predicted because of the solubility which depends to a certain degree on arrangement of molecules in the crystal and these topological aspects cannot be predicted via atom types or substructure fragments.

Table 5.6 preADME prediction of compounds.

Compound name	HIA%	Caco-2 nm/sec	MDCK nm/sec	In vitro plasma%	In vitro blood barrier
1a	96.73	25.98	0.04	93.29	0.135
2a	97.68	27.54	0.05	92.28	0.198
3a	98.06	37.28	35.19	96.43	1.137
3b	98.66	42.28	34.16	95.64	2.05
3c	96.94	45.54	0.053	96.39	2.34
3d	98.38	44.77	0.046	93.71	1.12
3e	98.53	44.77	0.020	96.49	2.31
3f	96.72	34.45	26.32	96.63	1.76
3g	97.68	36.43	26.46	97.18	1.96
3h	97.89	36.49	0.020	98.6	1.45
3i	97.589	36.55	32.52	99.18	2.28
3j	96.34	42.27	0.04	98.42	2.41
4a	98.06	38.752	15.94	96.47	0.84
4b	99.142	42.6359	0.044	93.484	0.027
4c	97.68	47.7122	0.044	92.11	0.135
4d	97.84	35.998	44.058	93.244	2.07
4e	98.06	17.55	25.09	96.07	1.107
4f	98.06	17.34	34.26	95.998	2.05
4g	97.62	43.077	0.182	93.022	0.269
4h	97.668	37.517	0.044	93.718	0.127
4i	97.589	37.62	0.0958	96.408	2.31
4j	97.589	37.62	0.053	100	1.39
4k	97.589	18.775	0.046	99.18	0.996
4l	97.63	42.27	0.020	100	0.1945
4m	97.809	38.752	0.094	100	1.319
4n	98.003	42.6359	0.0412	100	0.79

4o	98.033	47.7122	0.125	100	1.38
4p	97.592	35.998	0.025	98.44	0.491
4q	99.14	17.55	0.023	100	0.292
4r	99.143	17.34	0.0208	100	0.201
4s	97.64	43.077	0.021	98.35	0.159
4t	97.485	37.517	0.024	95.31	0.241
4u	97.485	37.62	0.026	92.21	1.88
4v	97.485	37.62	0.028	92.71	1.93
4w	99.38	18.775	0.0323	100	0.194
4x	96.169	21.197	0.138	94.513	0.623
4y	97.48	37.06	0.028	89.708	0.358
4z	96.56	22.355	0.037	98.24	0.49
4	97.64	39.17	75.66	91.17	1.67

5.3.2 Molecular Docking and Pharmacophore study

In order to evaluate the candidature of compounds as inhibitor of hDHFR, in terms of their binding affinity to hDHFR active site, we have performed molecular docking of these compounds with hDHFR. The protein-ligand complex structures were suitable for the docking study, since the ligand pockets were clearly determined.The docked complexes of receptor and compounds have been compared with the original PDB structure (1DHF:A) in terms of the occupancy of the active site by the compounds. The molecular alignment results (Figure 5.5) have shown that all the compounds under study along with the standard drug methotrexate have occupied the same cavity as is occupied by the natural ligand folate.

The active site of the human dihydrofolate reductase (hDHFR) is represented by Ile-7, Ala-9, Trp-24, Glu-30, Gln-35, Asn-64, Arg-70, Val-115, Tyr-121 and Thr-136 (Yamini *et al.,* 2011) as shown in Figure 5.6. It can be inferred that the compounds have affinity for the active site and can act as competitive inhibitors to the natural ligand.

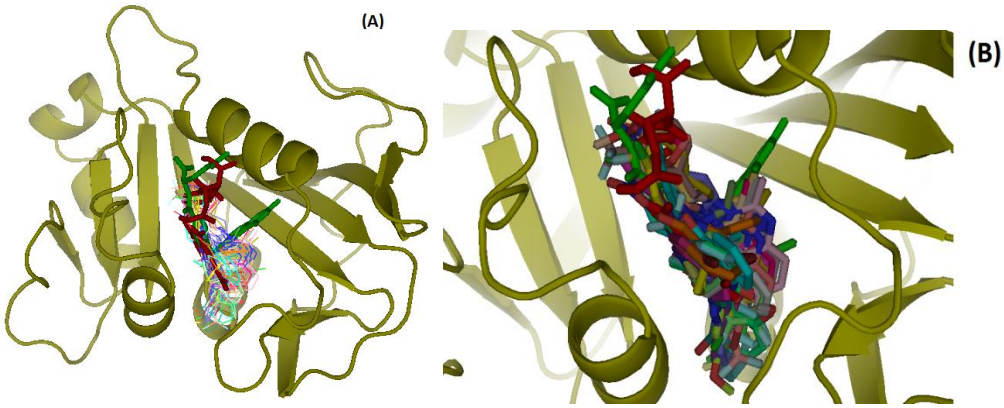

Figure 5.5: Docking model of compounds with hDHFR (PDB ID- 1DHF) protein (Folic Acid and methotrexate are represented in green and red sticks respectively, and the other molecules are shown in line representation) (B) Zoomed view of the active site showing all the docked molecules (ligands are represented in different color sticks including folic acid and methotrexate represented in green and red sticks respectively)

The compounds were evaluated in terms of their binding mode to hDHFR. Based on the Binding Free Energy (ΔG binding) of the protein-ligand interaction and Inhibition constant (Ki), one of 10 models was chosen to be the best one (Table 5.7). The docking result showed that all compounds have low binding energy and inhibition constant as compared to the standard drug methotrexate. The minimum binding energy (maximum stability) was found for compound 4e (-12.38 Kcal/mol). The N1 of 4e forms hydrogen bond with the Ser-59 with a distance of 2.71Å. The amino acids Val-115, Phe-31, Phe-34, Tyr-121, Thr-136 and Asp-21 are found to be involved in making hydrophobic interactions with 4e. Interestingly, all these amino acids are also present in active site of hDHFR, which infers that 4e binds in the active site region of enzyme. 4b molecule also formed significantly stable complex on docking. Similar to 4e, the N1 atom of 4b formed hydrogen bond with the Ser-59. It was reported that the tested quinazoline's recognition with the key amino acid Glu-30 and Ser-59 is essential for binding and biological activity (Al-Rashood *et*

al., 2006) The maximum binding energy was found in 4p (-10.05 Kcal/mol) which did not form hydrogen bond with the residues of the receptor.

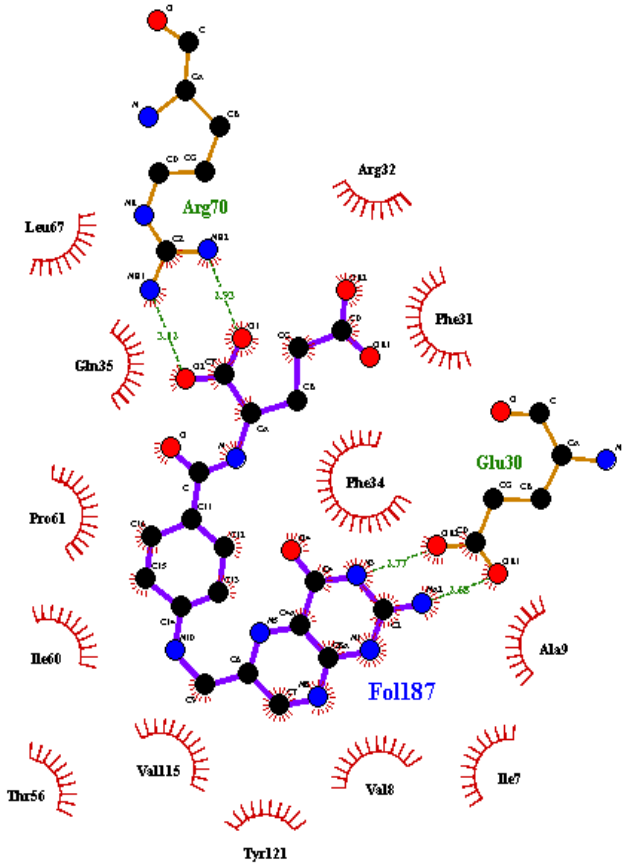

Figure 5.6: LigPlot generated snapshot of the residues in the active site of 1DHF interacting with the natural ligand Folate.

‘

It was observed from the calculated binding energies that incorporation of phenyl at 2-C increased the interaction with the enzyme in comparison to compounds substituted with methyl at 2-C. The compounds 4a- 4h have binding energies in range of -11.28 to -12.38 Kcal/mol. The inhibition constant is directly proportional to the binding energy as shown in Table 5.7. The docking model of compounds and hDHFR are shown in Figure. 5.7.

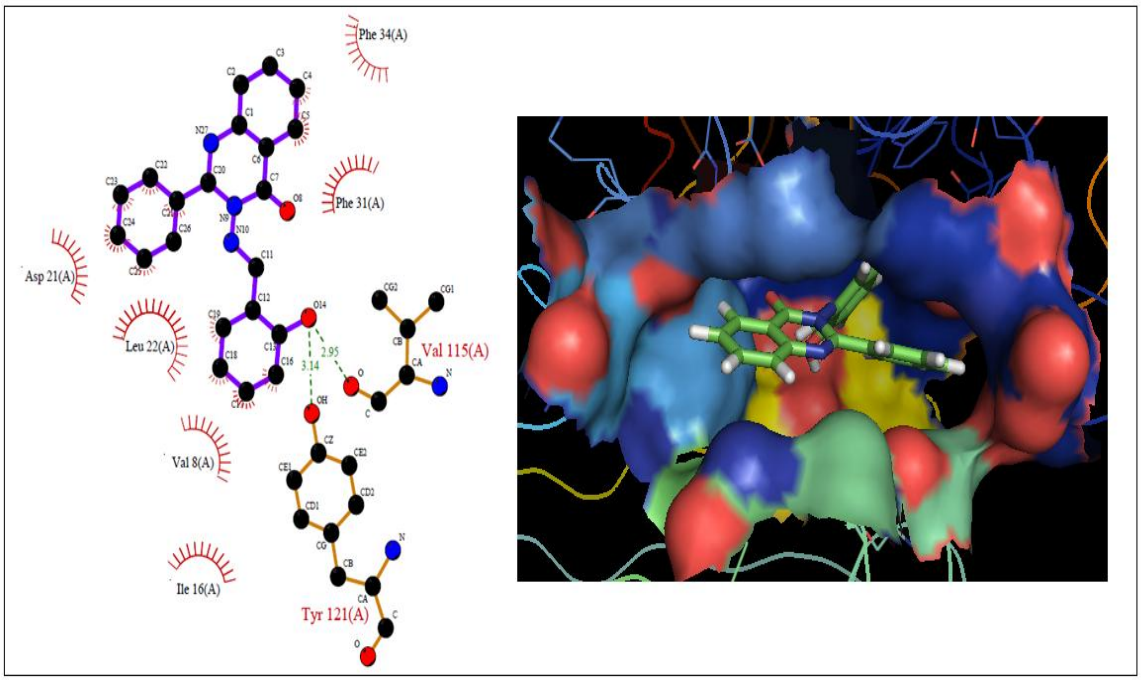

Figure 5.7 (a): Interaction of compound 3a docked with hDHFR

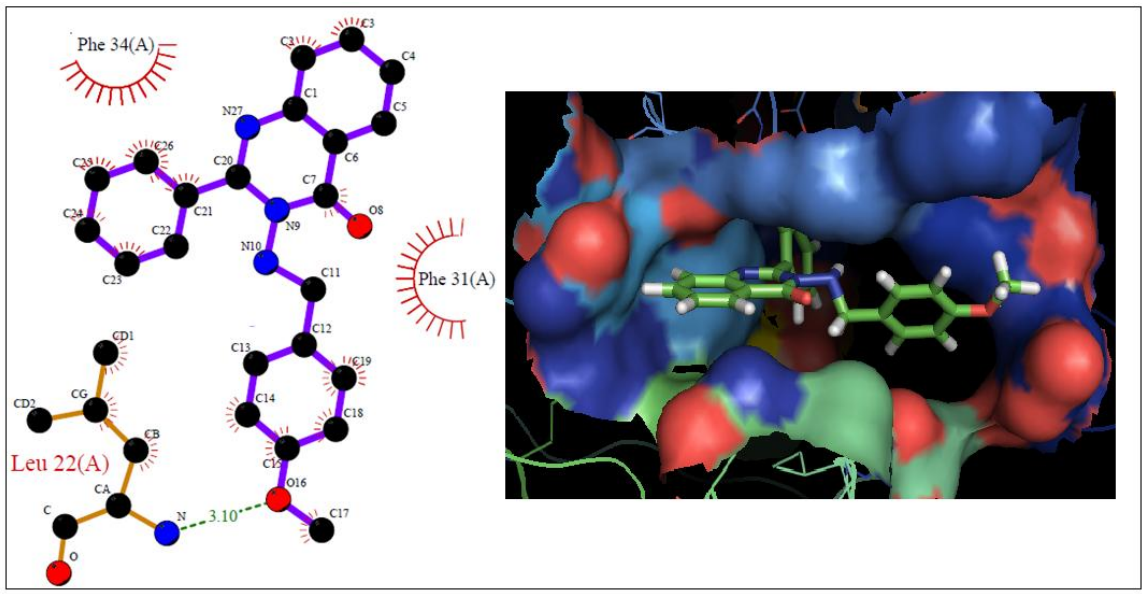

Figure 5.7 (b): Interaction of compound 3b docked with hDHFR

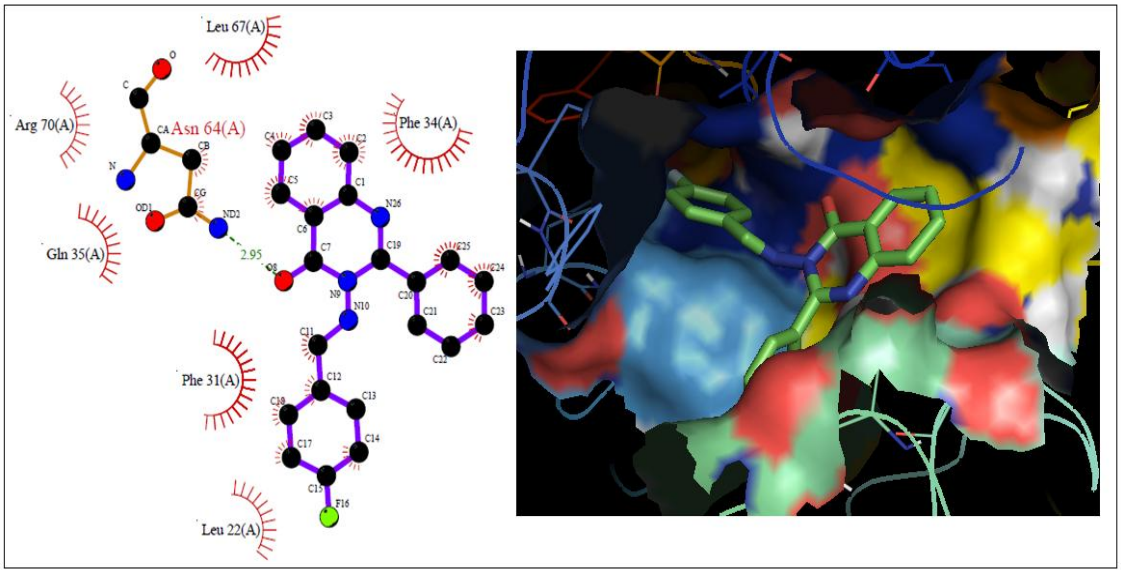

Figure 5.7 (c): Interaction of compound 3c docked with hDHFR

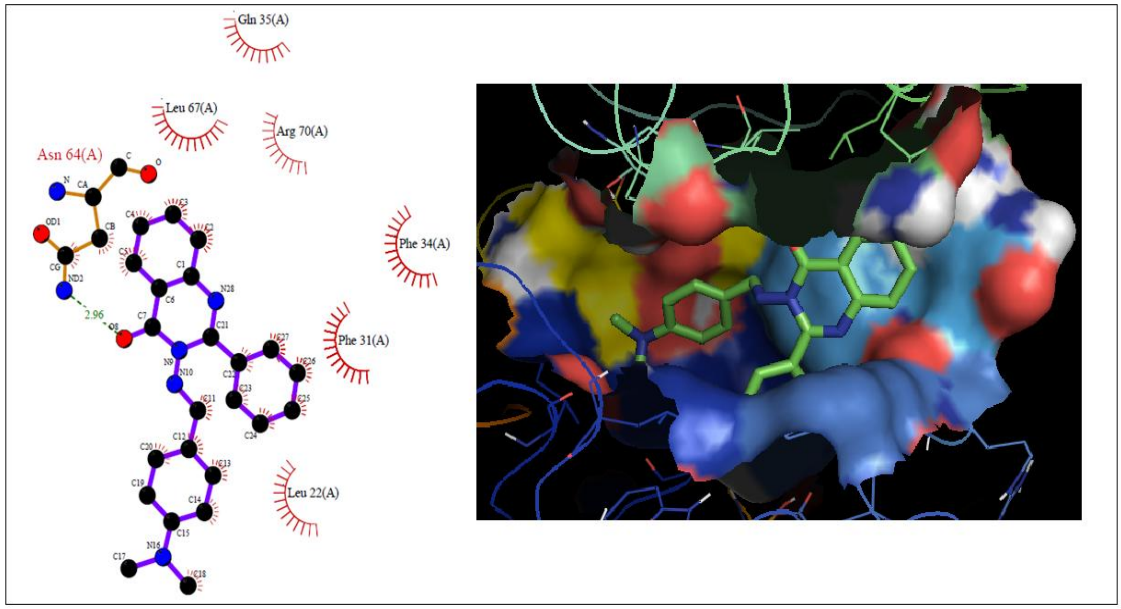

Figure 5.7 (d): Interaction of compound 3d docked with hDHFR

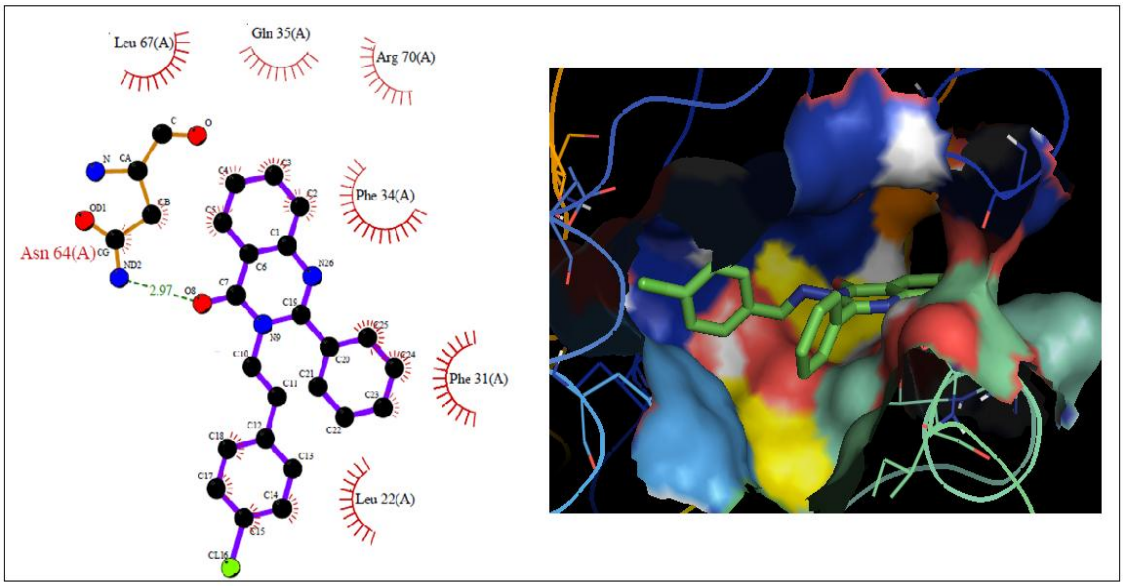

Figure 5.7 (e): Interaction of compound 3e docked with hDHFR

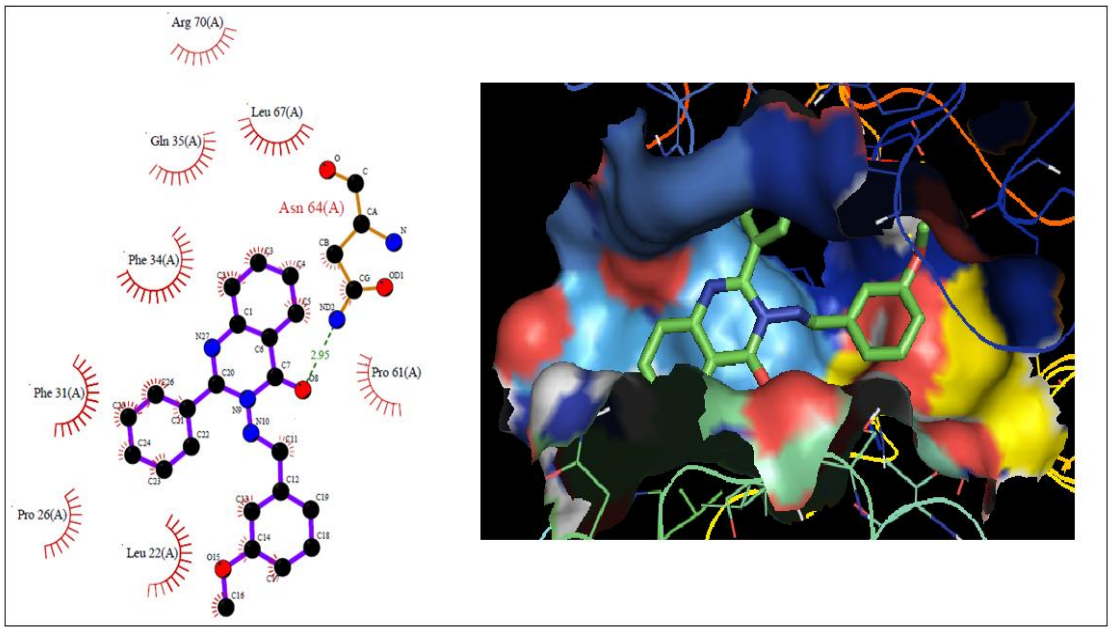

Figure 5.7 (f): Interaction of compound 3f docked with hDHFR

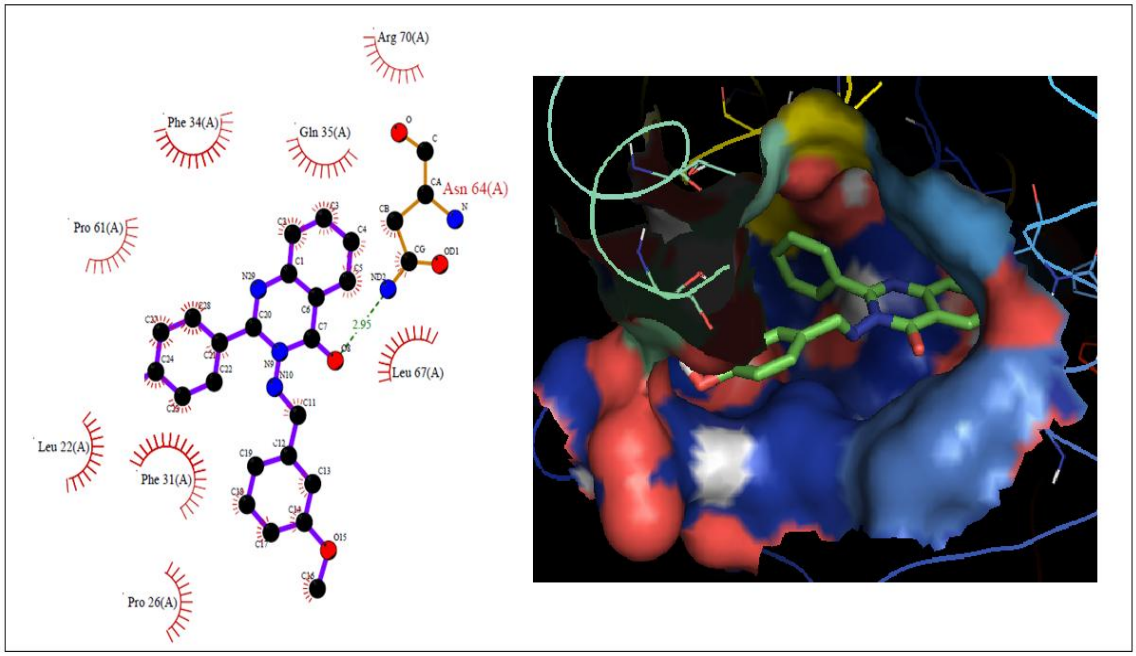

Figure 5.7 (g): Interaction of compound 3g docked with hDHFR

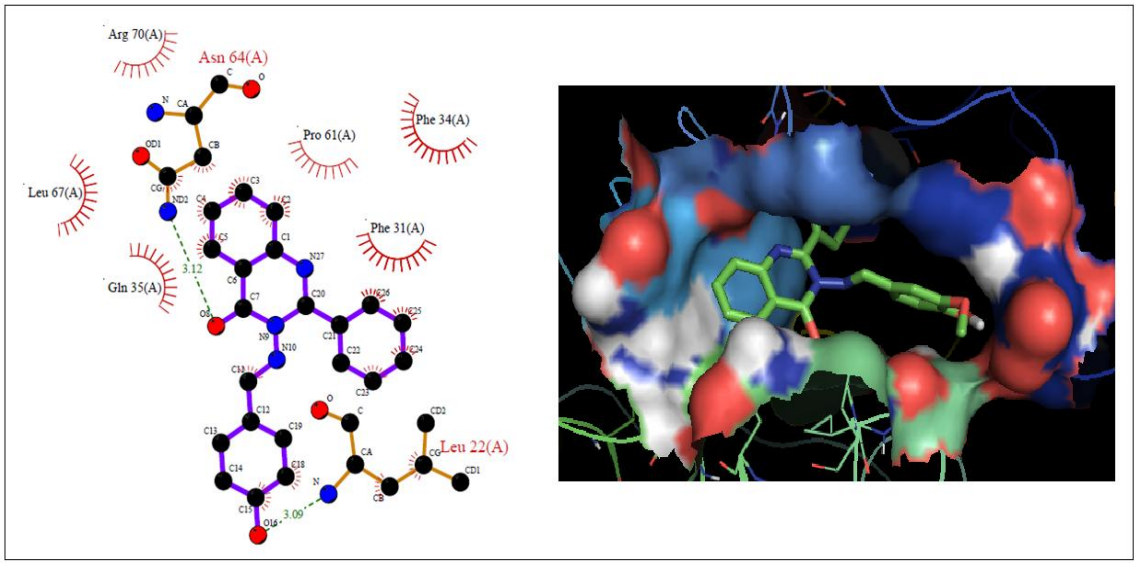

Figure 5.7 (h): Interaction of compound 3h docked with hDHFR

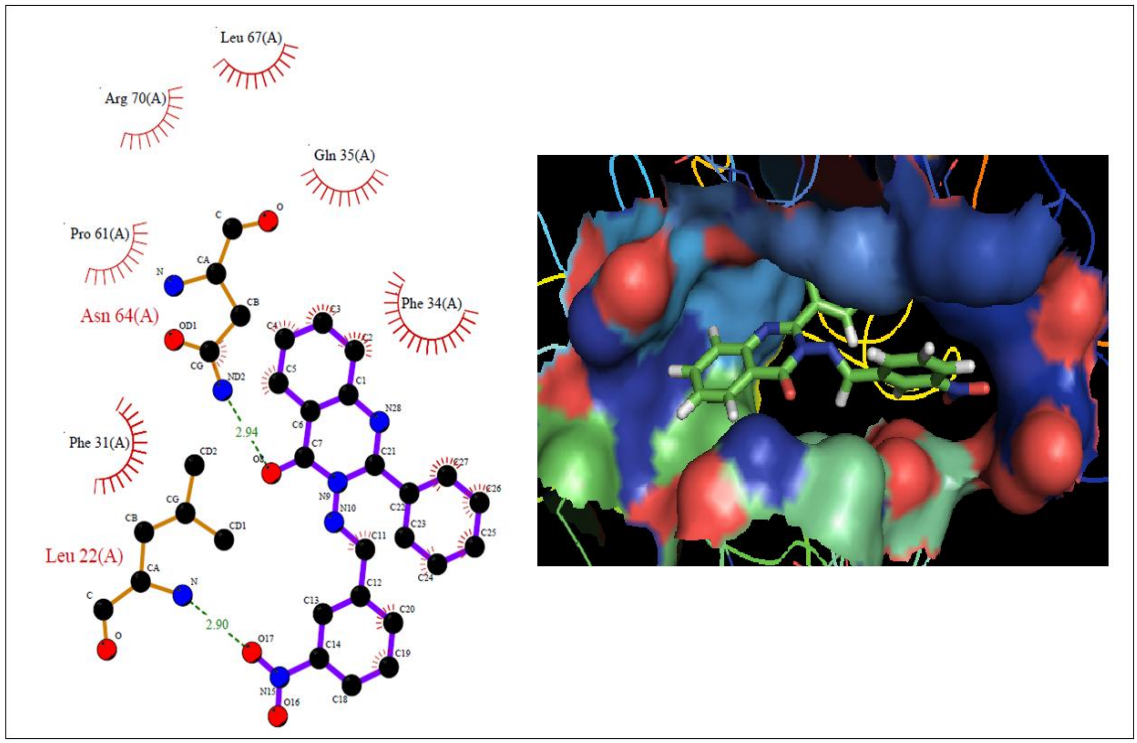

Figure 5.7 (i): Interaction of compound 3i docked with hDHFR

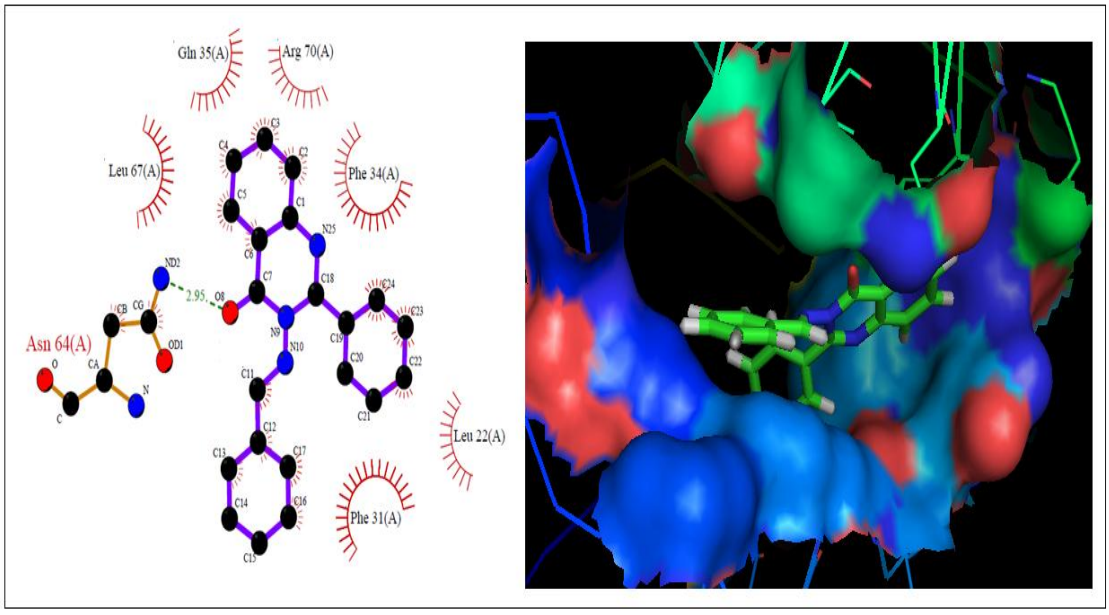

Figure 5.7 (j): Interaction of compound 3j docked with hDHFR

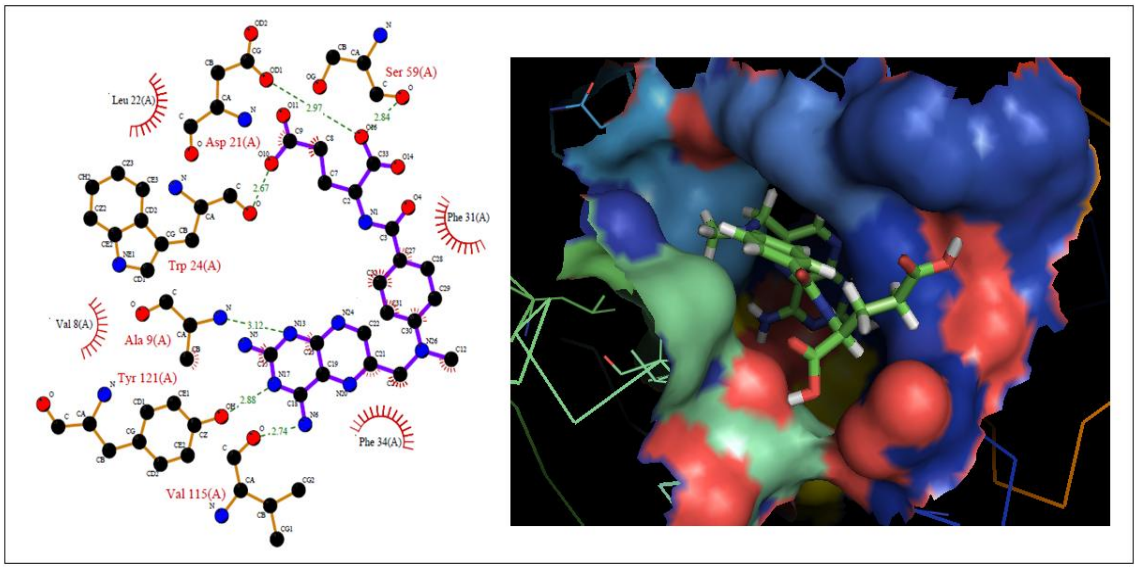

Figure 5.7 (k): Interaction of methotrexate docked with hDHFR

Table 5.7 Binding energy and Inhibition constant of ligand -human DHFR interaction for each test compound.

Compound	Binding energy Kcal/Mol	Inhibition constant (nM)
1a	-6.43	234µM
2a	-7.23	178 µM
3a	-10.62	16.38
3b	-10.79	12.28
3c	-10.43	22.64
3d	-11.17	6.42
3e	-10.89	13.96
3f	-10.72	10.13
3g	-10.91	31.21
3h	-10.24	10.21
3i	-11.62	3.2

3j	-11.37	4.64
4a	-11.73	2.5
4b	-12.33	0.91
4c	-11.2	6.61
4d	-11.7	2.35
4e	-12.38	0.846
4f	-11.88	1.96
4g	-11.26	5.55
4h	-11.28	5.43
4i	-10.45	21.82
4j	-10.65	15.49
4k	-10.62	16.23
4l	-10.96	9.26
4m	-11.14	6.79
4n	-11.39	4.44
4o	-10.76	13.0
4p	-10.05	42.94
4q	-11.52	3.59
4r	-11.5	3.72
4s	-10.56	18.06
4t	-10.41	10.09
4u	-10.92	9.91
4v	-10.56	18.18
4w	-12.15	1.23
4x	-10.79	12.35
4y	-10.62	16.35
4z	-10.38	24.81
4	-10.47	21.25
MTX	-8.62.	479.78

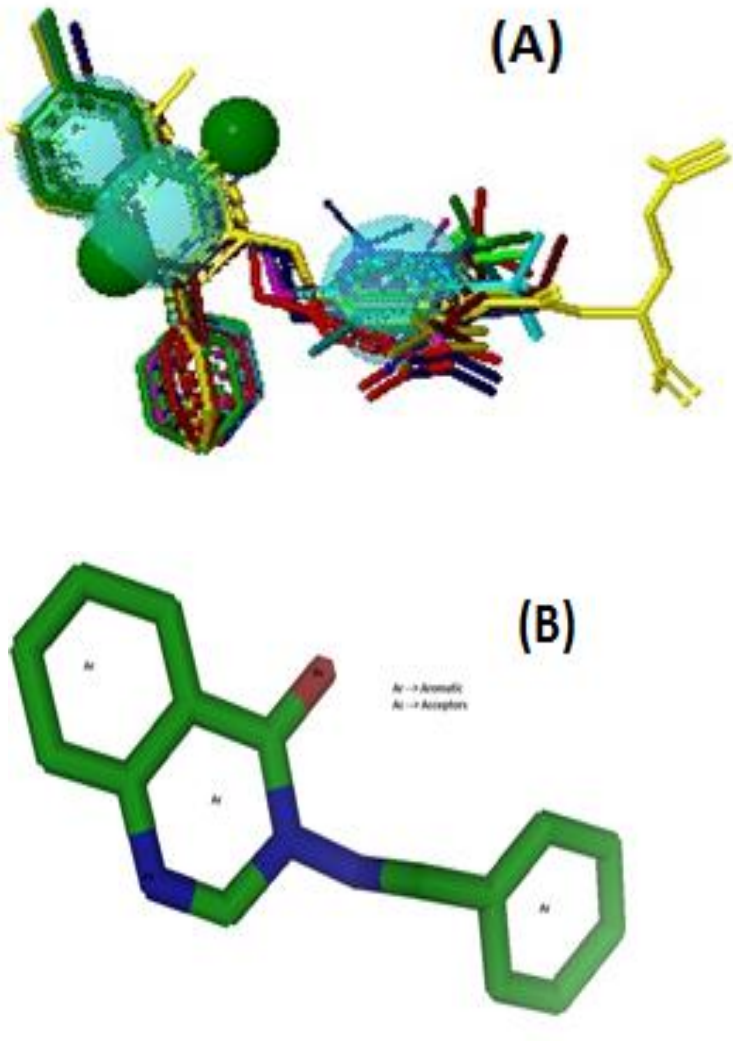

Figure 5.8: (A) Structural Alignment of molecules. (B) Pharmacophore having characteristics: Score(66.813)

The synthesized compounds have been comparatively evaluated in terms of their binding mode to hDHFR pocket. The substitution of 4th position with oxygen plays a vital role in binding with hDHFR. The most active compounds among 3 series 3i, in addition to Asp 64, it also forms hydrogen bond with Arg 70. The overall outcome of this molecular study revealed that: (1) the quinazoline ring is a satisfactory backbone for inhibition of mammalian DHFR, establishing contact with the key amino acids residues

in the enzyme pocket. The oxygen present at the 4th position formed hydrogen bond with the Asp 64 of hDHFR.

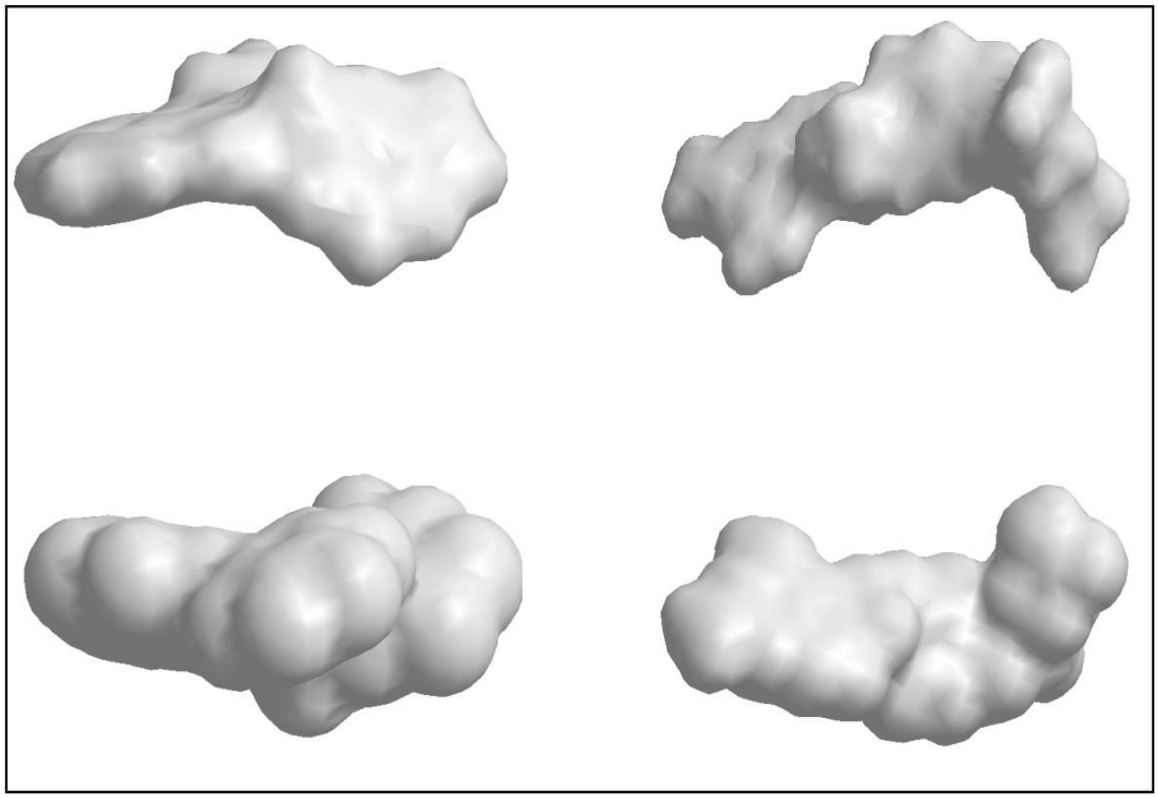

Figure 5.9: Connolly molecular surface (upper panel) and solvent accessible surface (lower panel) of MTX, 1 (left) and the active compound 3a (right).

Many authors have used ligand-based approach for pharmacophore modeling of species-specific DHFR inhibitors. Moreover, a pharmacophore model for hDHFR (human) inhibitors has also been modeled (Al-Omary *et al.,* 2010). All the studied compounds were used to develop a ligand based pharmacophore (Figure 5.8) using PharmaGist tool, which could be used further for the development of new, improved and optimized drug acting as inhibitor to hDHFR. The aligned binding conformation of the docked complexes clearly revealed that they can bind at the site quite well where natural ligand Dihydrofolate (Dhf) and inhibitor Methotrexate bound.

The pharmacophore has 3 aromatic rings and two hydrogen bond acceptors which enables in making several non covalent interactions like hydrophobic-hydrophobic interactions, hydrogen bonding, pi cloud interactions, etc.

This pharmacophore is qualifying all the four parameters of Lipinski's rule of five and thus could be considered as a lead molecule to generate new conformations for virtual screening library along with more modifications which could enhance its therapeutic index by enhancing the kind of interactions it could possibly make with the target protein. Furthermore, Connolly molecular surface, solvent accessible surface demonstrated their closely related molecular surface, charge distribution and electrostatic potential (Figure 5.9).

5.3.3 *In vitro* Inhibtion of Human Dihdrofolate reductase

The above section has shown that these compounds have possible properties and fragments to develop into a drug in future. We also found in molecular docking that these compounds have strong affinity for hDHFR. Hence, we thought to test the efficacy of these compounds as hDHFR inhibitors. Moreover, it is well known that amongst various methods of cancer treatment, inhibition of human dihydrofolate reductase plays a key role in cancer chemotherapy. Literature supports candidature of Quinazoline and quinazolinone to be potent hDHFR enzyme inhibitor hence chosen for this study. The synthesized compounds (3a-3j) were evaluated as inhibitors of human DHFR using instruction provided in assay kit. The human DHFR inhibition activities were reported as IC_{50} values (Tables 5. 8). Compounds 3a, 3d, 3g, 3h and 3i, proved to be the most active hDHFR inhibitors with IC_{50} values range of 0.3 to 5µM, while compounds 3b, 3c, 3e and 3f were considered of moderate activity with IC_{50} range of 6 to 10 µM, the rest of the tested compounds were considered poorly active with IC_{50} > 10 µM. Methotrexate (IC_{50} = 8 µM) was used as a positive control.

The inhibition in hDHFR activity indicated the inhibition of purine biosynthesis. The reference compound methotrexate showed IC_{50} value of 8±1.34, which is similar with the previous reports. The compounds 3a, 3b, 3c, 3d, 3f, 3g, 3h and 3i showed IC_{50} value less than methotrexate. Among these compounds, 3d and 3g showed four times less IC_{50} value than methotrexate.

Table 5.8- IC_{50} value of quinazoline-4(3H) against the hDHFR.

Compounds	hDHFR IC_{50} (μM)
3a	6.57±1.23
3b	8.0±0.53
3c	5.7±0.37
3d	2.4±0.41
3e	13.18±1.63
3f	7.87±0.82
3g	2.8±0.36
3h	5.95±1.53
3i	3.84±0.29
3j	17.21±0.64
MTX	8±1.34

5.3.4 Antiproliferative activity

As we have mentioned that our main focus of this chapter was to propose the antiproliferative activity of 3-(Aryldeneamino)-2-phenyl-quinazoline-4(3H)-one. Generally, for an agent to be useful as an anti-cancer drug, it must show preferential anti-proliferative activity against tumor cell lines. All the synthesized compounds (1a, 2a and 3a-3j) along with Methotrexate and curcumin (as a reference drug) were screened for their antitumour activity against three cancerous cell lines; HepG2 (human liver cancer cell line), MCF-7 (human breast cancer cell line) and HeLa (human cervical cancer cell line) using MTT assay as described previously with slight modification. Each cell line was incubated with five concentrations (0–100 μg/mL) of each compound and the results were used to create compound concentration versus survival fraction curves. Three experiments with test compounds were performed in triplicate for each assay and the percent inhibition of cell viability was determined and compared with the data available for standard Methotrexate and Curcumin. The data were subjected to linear regression analysis and the regression lines were plotted for the best fit straight line. The IC_{50} (50%

inhibition of cell viability) concentrations were calculated based on the regression equation. The IC_{50} of each compound against cell lines are shown in Table 5.9.

The results represented in Figures 5.10, 5.11 and 5.12 clearly show the growth inhibitory effect in HeLa , HepG2 and MCF7 cell lines in the presence of synthesized compound at concentration of 75µg/mL .

Table 5.9: IC_{50} value of quinazoline-4(3H) against the growth of HeLa, HepG2 and MCF7 cancer cell lines.

Compounds	HeLa (µg/ml)	MCF 7 (µg/ml)	HepG2 (µg/ml)
1a	ND	ND	ND
2a	ND	ND	ND
3a	22±2	21±6	23±3
3b	97±5	ND	28±5
3c	ND	95±5	45±3
3d	54±3	68±3	ND
3e	87±6	ND	ND
3f	ND	ND	30±4
3g	ND	52±5	64±6
3h	ND	ND	27±4
3i	23±4	28±5	46±4
3j	ND	ND	ND
Curcumin	17±1	22 ±3	9±3
Methotrexate	27±2	29±2	42±3.7

ND- Not Defined

So, concerning sensitivity of cell lines to the synthesized compounds, HepG2 cell line was shown to be the most sensitive toward the tested compounds followed by MCF7 and HeLa cell lines. Out of the 12 compounds, 7 showed activity against HepG2 cell lines, 5 showed against MCF7 cell line and 5 showed against HeLa cell lines. So, the tested compounds showed a distinctive pattern of selectivity. Based on the IC_{50} values, we have categorized the active compounds in three groups; highly active compounds

whose IC_{50} ranges from 0-30 μg/mL, moderate active compounds whose IC_{50} ranges from 31-70 μg/mL and poor active compounds whose IC_{50} ranges from 71-100 μg/mL.

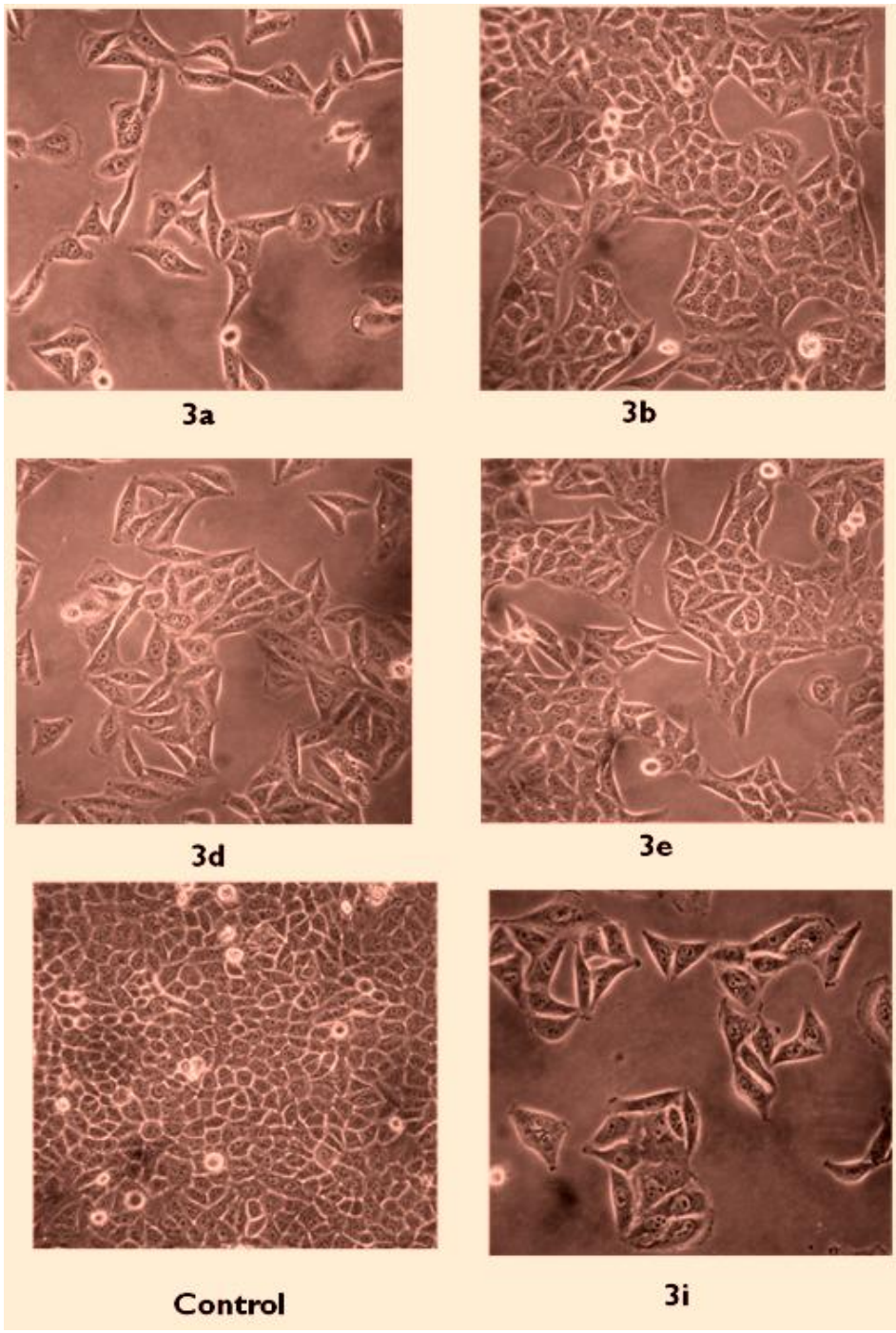

Figure 5.10: Effect of 75μg/ml of quinazoline-4(3H)-one on the proliferation of HeLa cell line (observed under phase contrast microscope).

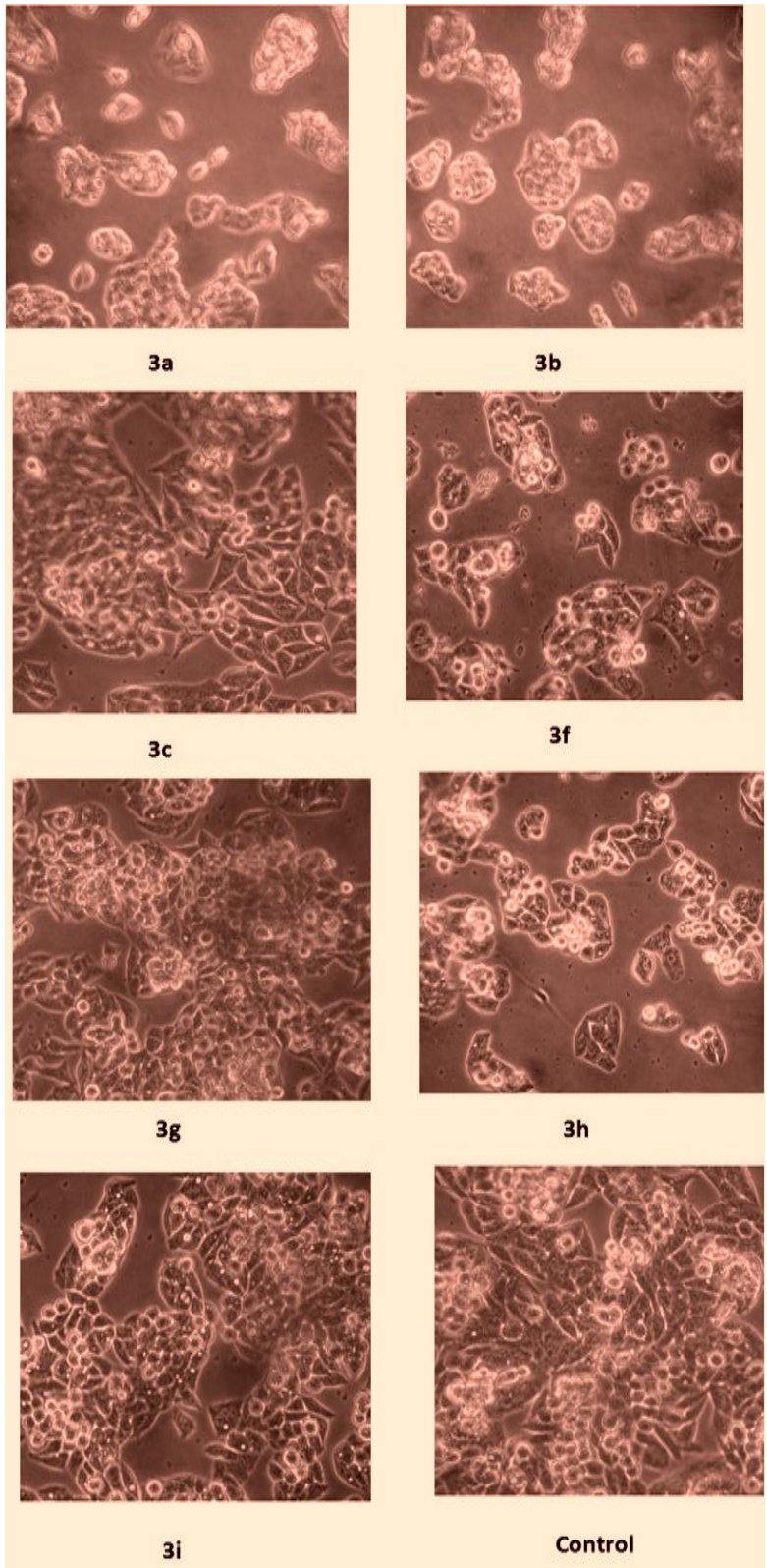

Figure 5.11: Effect of 75µg/ml of quinazoline-4(3H)-one on the proliferation of HepG2 cell line (observed under phase contrast microscope).

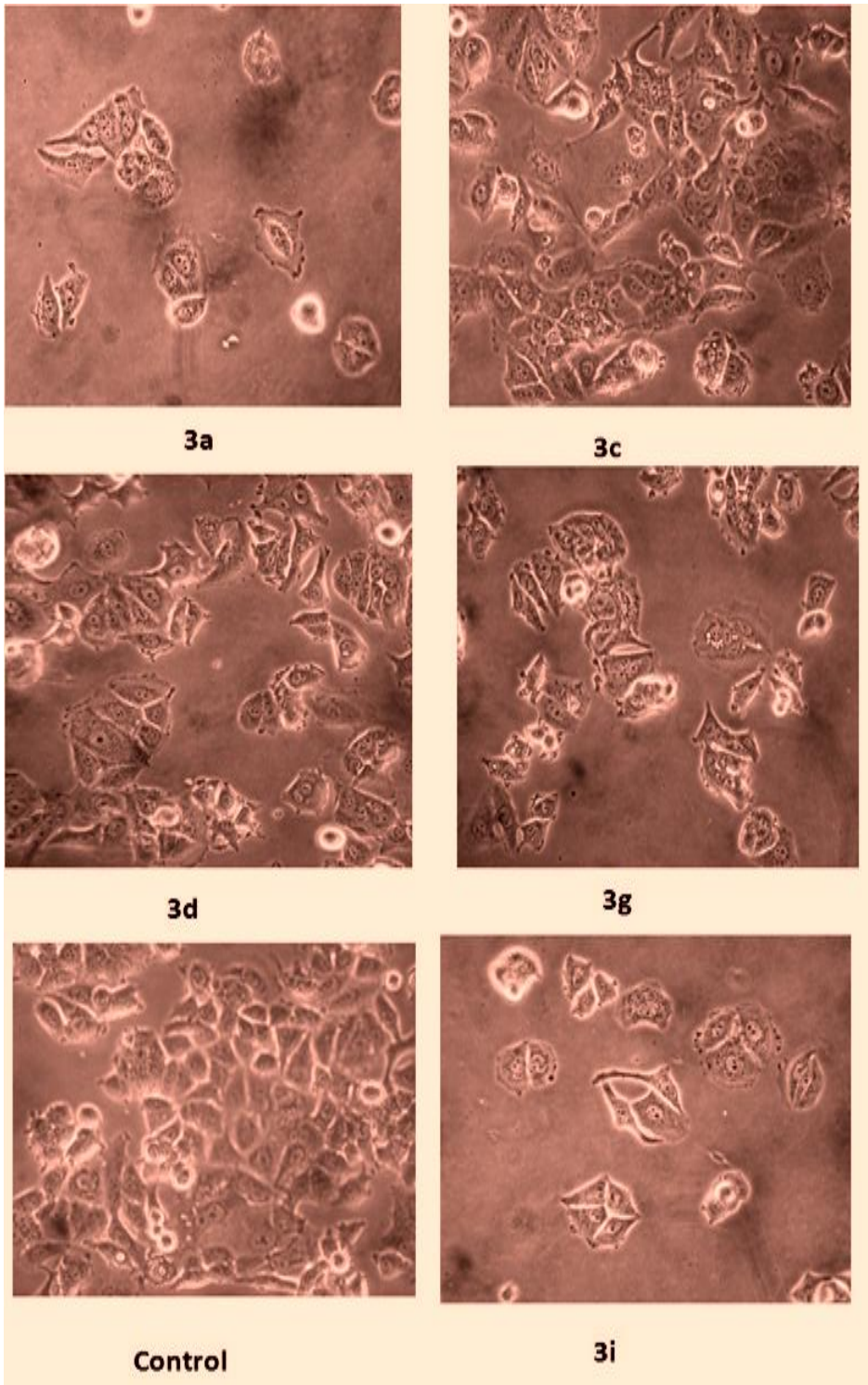

Figure 5.12: Effect of 75µg/ml of quinazoline-4(3H)-one on the proliferation of MCF7 cell line (observed under phase contrast microscope).

Considering HepG2 cell line, compound 3a (IC_{50} = 23±3) showed highest activity, along with 3a, 3b, 3f and 3h showed high activity, 3c and 3i showed moderate activity while 3g (IC_{50} = 64±6) shows poor activity. Against MCF7 cell line, compound 3a (IC_{50} = 21±6), 3i (IC_{50}= 28±5) showed high activity, 3d and 3g showed moderate activity whereas, 3c (IC_{50}= 95±5) showed poor activity. In view of HeLa cell line, compound 3a and 3i showed high activity, 3d showed moderate activity while 3b and 3e showed poor activity. Results revealed that 3a and 3i showed broad spectrum activity by inhibiting the proliferation of three studied cell lines. The broad spectrum activity of compound 3i could be related to presence of a nitro-aromatic group in the 2- phenylquinazolinone ring system. Various literatures supported that nitro group containing compounds showed various biological activities like antibacterial, antihelmentic, anticancer etc. Previous author reported that presence of nitro group enhanced the cytotoxicity activity in human melanoma cell (Sk *et al.,* 2011). The nitro-aromatic compound, 1-chloro-2,4-dinitrobenzene (dinitrochlorobenzene, DNCB) has been reported to induce apoptosis in HeLa and A549 cells (Cennas *et al.,* 2006). The nitro group containing aromatic compound, Flutamide, is also used in metastatic prostate cancer (Coe *et al.,* 2007). Aromatic compounds containing hydroxyl group is reported to regulate biological activities. The methoxy group present in the aromatic ring was also reported to possess vital role in growth inhibition activity (Nagarajan *et al.*, 2004). Curcumin containing hydroxy and methoxy groups were shown to possess higher cytotoxic activity on different cell lines (Naama *et al.*, 2010). Compound 3g contains both hydroxyl and methoxy groups in its quinazolinone ring, the presence of these two groups may be responsible for its effect on the cancer cell lines used. The hydroxyl group present in the compound in 3a may be attributed to its higher activity. So, we can hypothesize that the high activity of compounds 3a and 3i against three cancer cells may be attributed to the occurrence of OH and NO_2 moieties which may be important for hydrogen bonding at the receptor site. The results obtained from trypan blue test were similar to those obtained by the MTT test and reveal a clear cytotoxic effect of these compounds. Morphological alterations, such as rounded cells were not visible after 24 of incubation. Interestingly, the extent of the cytotoxic effects of the compounds depended on the tumour cell line.

These compounds also exhibited several interactions with human dihydrofolate reductase enzyme, giving rise to the conclusion that they might exert their action through inhibition of hDHFR enzyme. However, the same pattern of inhibition was not observed in antiproliferative activity. This may be due to the hindrance in entrance and bioavailability of compounds. We have addressed the way out of low solubility in the next chapter.